2014

Novel plant oil-based thermosets and polymer composites

Kunwei Liu
Iowa State University

Novel plant oil-based thermosets and polymer composites

by

Kunwei Liu

A thesis submitted to the graduate faculty

in partial fulfillment of the requirements for the degree of

Master of Science

Major: Materials Science and Engineering

Program of Study Committee:
Samy Madbouly, Co-major Professor
Nicola Bowler, Co-major Professor
Vinay Dayal
Larry Genalo

Iowa State University

Ames, Iowa

2014

TABLE OF CONTENTS

LIST OF TABLES iv

LIST OF FIGURES v

ACKNOWLEDGEMENTS viii

CHAPTER 1 : GENERAL INTRODUCTION 1

1.1 Thesis Organization 1

1.2 Background and Literature Review 2

1.2.1 The petroleum crisis and future trends of vegetable oil-based polymers 2

1.2.1 Vinyl polymers derived from vegetable oils 5

1.3 Objectives 14

1.4 Reference 14

CHAPTER 2 : BIO-BASED THERMOSETTING POLYMER BASED ON SOYBEAN OIL AND EUGENOL 19

2.1 Abstract 19

2.2 Introduction 20

2.3 Experiment Details 24

2.3.1 Materials 24

2.3.2 Synthesis of methacrylated eugenol 24

2.3.3 Free radical polymerization of AESO/ME copolymers 25

2.3.4 Material Characterizations 26

2.4 Result and Discussion 28

2.4.1 Synthesis of AESO/ME copolymers 28

2.4.2 NMR 30

2.4.3 Soxhlet extraction 33

2.4.4 Rheological properties 33

2.4.5 Thermal properties 36

2.4.6 Compression testing 41

2.5 Conclusion 44
2.6 Acknowledgements 45
2.7 References 45
CHAPTER 3 : BIORENEWABLE POLYMER COMPOSITES FROM TALL OIL-BASED POLYAMIDE AND LIGNIN-CELLULOSE FIBER 50
3.1 Abstract 50
3.2 Introduction 51
3.3 Experimental Procedure 55
3.3.1 Materials 55
3.3.2 Composite Preparation 56
3.3.3 Morphological characterization 56
3.3.4 Optical Microscopy 57
3.3.5 DMA measurements 57
3.3.6 DSC measurements 57
3.3.6 TGA measurements 58
3.3.7 Rheological measurements 58
3.3.8 Mechanical testing 58
3. 4 Results and Discussion 59
3.4.1 Optical microscopy and SEM 59
3.4.2 Rheology 60
3.4.3 DMA 63
3.4.4 DSC 65
3.4.5 TGA 66
3.4.6 Mechanical testing 70
3.4 Conclusions 73
3.5 Acknowledgements 73
3.6 References 73
CHAPTER 4: GENERAL CONCLUSION 78
4.1 Summary 78
4.2 Recommendation for future works 80
4.3 Reference 83

LIST OF TABLES

Table 1-1: Chemical structures and formulas for some common fatty acids [9, 10]..... 7

Table 2-1: Soxhlet extraction data for all copolymers..... 33

Table 2-2: Glass transition temperature and storage modulus at room temperature. The glass transition temperatures is obtained from the maxima the tan δ curves obtained by DMA analysis. 38

Table 2-3: Important thermal degradation temperature for AESO/ME copolymers. 41

Table 3-1: Important degradation temperature obtained from TGA. 69

LISTS OF FIGURES

Figure 1-1: Chemical structure of triglycerides. 6

Figure 1-2: Chemical structures of styrene, divinylbenzene, soybean oil and their copolymers produced by cationic polymerization [17]. 9

Figure 1-3: Synthesis of soybean oil monoglyceride maleates and copolymerization with styrene [28]. 12

Figure 2-1: Synthesis of acrylated epoxidized soybean oil (AESO). 22

Figure 2-2: Synthesis of methacrylated eugenol. 26

Figure 2-3: The crosslinking reaction between AESO and ME. 29

Figure 2-4: ^{1}H NMR spectrum of as-received eugenol. 31

Figure 2-5: ^{1}H NMR spectrum of methacrylated eugenol. 32

Figure 2-6: ^{1}H NMR spectrum of acrylated epoxidized soybean oil. 32

Figure 2-7: Gelation time for AESO/ME copolymers with different compositions cured at 70°C, 80°C, and 90°C. 35

Figure 2-8: Viscosity of AESO/ME copolymers as a function of shear rate. 36

Figure 2-9: Storage moduli for AESO/ME copolymer with different chemical compositions. 37

Figure 2-10: Tan δ curves for AESO/ME copolymers with different chemical compositions. 39

Figure 2-11: TGA measurements for AESO/ME copolymers with different compositions at 20°C/min heating rate under nitrogen atmosphere. 40

Figure 2-12: Compressive modulus for AESO/ME copolymers with different compositions. 42

Figure 2-13: Maximum compressive strength and compressive yield strength of AESO/ME copolymers with different compositions. 43

Figure 2-14: Maximum compressive strain for AESO/ME copolymers with different compositions. 43

Figure 3-1: Optical micrograph of LCF. 59

Figure 3-2: SEM images of the fracture surfaces of (a) PA-0%; (b) PA-10%; (c) PA-20%; PA-30%. 60

Figure 3-3: Angular frequency dependence of storage modulus at 140°C for PA/LCF composites with different filler contents 62

Figure 3-4: Angular frequency dependence of complex viscosity at 140°C for PA/LCF composites with different filler contents 62

Figure 3-5 : Storage modulus as a function of temperature for the pure PA polymers and its composites with 10wt% to 30 wt% LCF 64

Figure 3-6: Tan δ curves as a function of temperature obtained via DMA. 65

Figure 3-7: DSC traces of PA polymer and composites containing 10 wt% to 30 wt% of LCF. 66

Figure 3-8: Thermal degradation behavior of pure PA polymer, the pure LCF, and their composites 68

Figure 3-9: Enlarged portion of Figure 3-8 showing details about the onset of thermal degradation. 68

Figure 3-10: Weight derivative of pure PA polymer, LCF, and their composites 69

Figure 3-11: Young’s modulus as a function of LCF content. 71

Figure 3-12: Yield Strength as a function of LCF content. 72

Figure 3-13: Strain at break as a function of LCF content. 72

ACKNOWLEDGEMENTS

First, I would like to thank Dr. Michael Kessler for providing me the opportunity to perform research in the Polymer Composite Research Group. Without his support and guidance, I would not be able to complete my graduate study. I would like to express my thanks to Dr. Samy Madbouly, who provided tremendous amount of guidance during my research. When I first joined the group, I knew almost nothing about polymers. Dr. Madbouly was always very patient when explaining some very basic knowledge to me. He also provided me a lot of technical guidances throughout my research work. In addition, I would also like to thank Dr. Nicola Bowler, Dr. Vinay Dayal, and Dr. Larry Genalo for serving on my advisory committee and providing technical guidances.

I have worked on several projects during my graduate studies. As a result, I would like to thank United Soybean Board, Siegwerk, and the Consortium for Plant Biotechnology Research (CPBR) for their financial support. I would also like to thank all current and previous members in the Polymer Composites Research Group and in the MSE office, including Hongyu Cui, Rui Ding, Hongchao Wu, Ruqi Chen, Yuzhan Li, Eliseo De León, Danny Vennerberg, Harris Handoko, Ying Xia, Rafael Gauri Ramasubramanian, Dana Akilbekova, Chaoqun Zhang, Mike Zenner, Shenze Yang, Hong Lu, James Bergman, Rafael Quirino, and Larrisa Fonseca for their friendships and technical assistances. Among them, I would like to specially thank Harris and Larrisa for teaching me the methacrylation of eugenol, which is essential for this thesis. In addition, I am grateful for the technical discussions provided by Danny Vennerberg, Ying Xia, and Rui Ding. I also want to thank Danielle Carda and Victor Lee, the undergraduates students who helped me perform

experiment. In addition, I appreciate Danielle Carda for time to revise the grammatical errors on my thesis.

At last, I wish to thank my mother, Bing Liang, my father, Shunyi Liu, and my girlfriend Chujun Liang for their continuous encouragements and supports.

CHAPTER 1 : GENERAL INTRODUCTION

1.1 Thesis Organization

The works presented in this thesis are written as manuscripts for academic journal publication. Chapter 1 discusses the current problems with the use of petroleum-based polymers and the future trends of biorenewable polymers. A literature research on vegetable oil-based vinyl polymers will also be presented. Chapter 2 includes a novel high bio-content thermosetting polymer based on acrylated epoxidized soybean oil and methacrylated eugenol. This resin system was intended to be a matrix resin for fiber reinforced composites produced by the pultrusion process. There are very few studies about developing vegetable oil-based polymers for pultrusion process (or even for other composite manufacturing procedures). This resin, to the best of my knowledge after searching the literatures, is the first vegetable oil-based thermoset with more than 70% biorenewable carbon content that are suitable for the pultrusion process. Chapter 3 presents a biocomposite based on tall oil-based polyamide as the matrix and lignin-cellulose fiber as fillers. These composites were studied using various material characterization techniques to understand the effects of lignin-cellulose fiber on the thermal, mechanical, and rheological properties of the final composites. Chapter 4 contains the overall summary of my thesis and some possible future research directions.

1.2 Background and Literature Review

1.2.1 The petroleum crisis and future trends of vegetable oil-based polymers

Because of the continuously increasing price of petroleum resources and an increase in environmental awareness, researchers are actively trying to produce polymeric materials based on biorenewable resources to replace the traditional petroleum-based plastics. Thermoplastics such as polyethylene, polypropylene, polystyrene, poly(vinyl chloride) and thermosets such as epoxies and polyesters are used everywhere in our daily life. The applications of plastic are essentially limitless. Some typical applications of plastics include packaging, textiles, coatings, automobile components, biomedical devices and household items. Our dependence on plastics keeps increasing, but the fossil fuel is depleting. It is proposed that all petroleum resources will be exhausted within the next one hundred years [1]. Nowadays, the price of fossil fuel and petroleum is still reasonable and affordable, thus many biorenewable polymers such as polylactide (PLA) and polyhydroxyalkanoates (PHA) cannot compete with traditional petroleum-based plastics in terms of cost. Many people are still not aware of the urgencies of developing biorenewable plastics because people can still afford pumping gasoline in their cars. Currently, due to the relatively high cost and inferior performance of biorenewable plastics, there is almost no incentive for industry to switch from traditional plastics to biorenewable plastics, even though biorenewable composites are more environmentally friendly. Fortunately, there have been some movements towards using biorenewable plastics in packaging applications. One of the examples is the PLA-based SunChips packaging. However, at high-tech applications such as the aerospace and military industries, biorenewable plastics are rarely seen.

It is important to continuously put research efforts into developing better biorenewable polymers because petroleum resources will eventually be depleted. In the future, biorenewable polymers with the following characteristics should be developed:

(1) Higher renewable content. In other words, the biorenewable resources should be kept as close to their original forms as possible, or the percentage of biorenewable carbons in the final products should be as high as possible. Most of the time, chemical modifications are performed on biorenewable resources to produce materials with better properties. Chemical modifications of these biorenewable resources normally require catalysts, solvents, and reagents; however, almost all catalysts, solvents and reagents are produced from petroleum resources. Another popular method to increase the properties of biorenewable polymers is by copolymerization with petroleum-based monomers. Take soybean oil as an example: soybean oil contains unconjugated carbon-carbon double bonds. Even though there are double bonds in soybean oil, free radical polymerization and cationic polymerization cannot be performed on soybean oil because unconjugated carbon-carbon double bonds in soybean oil are not reactive enough. To overcome the low reactivity problem of soybean oil, Li et al. has copolymerized soybean oil with styrene and divinylbenzene to produce materials with high rigidity [2]. In addition, Li et al. and Larock et al. also utilized homogeneous transition metal catalysts to transform regular soybean oil to conjugated soybean oil, which will have higher reactivity towards radical polymerization [3, 4]. Styrene was also used as a reactive diluent of acrylated epoxidized soybean oil (AESO) [5]. On the other hand, the term “bio-based” is

still vague in the field. Ma et al. prepared a thermosetting polymer based on rosin acid (one kind of biorenewable resource) and acrylated epoxidized soybean oil [6]. The author of this article utilized various petroleum-based chemicals, including acrylic acid, hydroquinone, and allyl bromide to modified rosin acid into divinyl acrylicpimaric acid [6]. Moreover, in this reaction process, the molar ratio of allyl bromide and rosin acid was about 3 to 1. Even though a lot of petroleum-based chemicals were used, the author of this article still claimed this thermoset as "full bio-based" materials. The materials developed by Ma et al., in my opinions, should be called "partially bio-based" instead of "full bio-based." In the future, biorenewable polymers with a minimal amount of petroleum contents should be developed.

(2) Lower price. Price is one of the most important aspects when selecting materials for a new design. It is difficult for a company to make a profit if a high-cost material is selected instead of a low-cost material. As mentioned previously, the current cost of biorenewable polymers is higher than those of petroleum-based polymers. If there are a biorenewable plastic and a petroleum-based plastic that can both satisfy the performance requirements of a component, the company will still choose to use the cheaper petroleum-based plastics. If low-cost biorenewable polymers can be developed, the industry will have a higher incentive to use this kind of environmentally friendly material.

(3) Higher performance. The mechanical properties of many biorenewable polymers are inferior to those of petroleum-based polymers. For example, the brittleness of PLA and PHA has limited their applications. If biorenewable polymers with

higher performance and reasonable cost can be developed, then there will be a higher incentive to use these sustainable and environmentally friendly materials.

(4) Reduce the use of petroleum-based catalysts and initiators. In order to turn monomers into polymers, most of the time, initiators have to be used in order to start the polymerization reaction. Most of the polymerization initiators such as free radical initiators or cationic initiators are derived from petroleum. One may argue that in a polymerization reaction, the percentage of initiator is very small. For most polymer systems, it is impossible to produce polymers without an initiator; but one has to keep in mind that if all the petroleum resources are depleted, it will become impossible to produce these initiators or catalysts. Studies have shown that it is possible to use thermal polymerization (use heat to polymerized monomer without an initiator) to produced vegetable oil-based thermosets [7].

1.2.1 Vinyl polymers derived from vegetable oils

In recent years, many vegetable oil-based polymers with a wide range of properties have been developed. Vegetable oils are attractive starting materials for preparing polymers because they are relatively cheap, commercially available, and most of them are not toxic to humans. Vegetable oils also contain many active functional groups, such as double bonds and hydroxyl groups, which can be chemically modified to produce polymers with desired properties. Vegetable oils are extracted from various plants, such as soybean, castor, tung tree, and palm tree. The general structure of vegetable oils is shown in Figure 1-1. Vegetable oils are made of triglycerides; that is, three separate fatty acid chains that connect to the glycerol backbone via ester linkage.

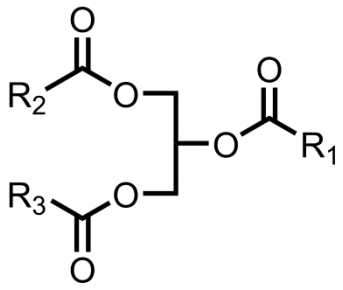

R_1,R_2,R_3 represents fatty acid chains

Figure 1-1: Chemical structure of triglycerides.

Some common fatty acids in vegetable oils are shown in Table 1-1. A fatty acid chain is a long chain consisting of 8 to 22 carbons, and some of them contain carbon-carbon double bonds, hydroxyl groups, and epoxy groups. A single type of vegetable oil contains multiple kinds of fatty acids. For example, soybean oil contains 11.0% palmitic acid, 4.0% stearic acid, 23.4% oleic acid, 53.3% linoleic acid, and 7.8% linolenic acid [8]. As a result, not every triglyceride molecule is the same. Vegetable oils are a mixture of triglycerides containing different fatty acid chains. This introduction will cover some vinyl polymers derived from vegetable oils; in other words, polymers produced from additional polymerization of carbon-carbon double bonds will be discussed.

Table 1-1: Chemical structures and formulas for some common fatty acids [9, 10].

Fatty Acid	Formula	Structure
Caprylic	$C_8H_{16}O_2$	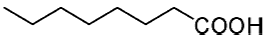
Capric	$C_{10}H_{20}O_2$	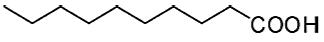
Lauric	$C_{12}H_{24}O_2$	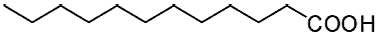
Myristic	$C_{14}H_{28}O_2$	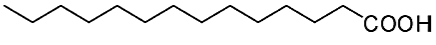
Palmitic	$C_{16}H_{32}O_2$	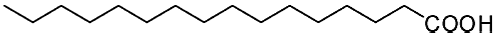
Palmitoleic	$C_{16}H_{30}O_2$	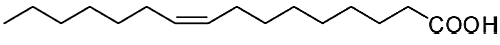
Stearic	$C_{18}H_{36}O_2$	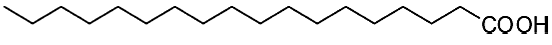
Oleic	$C_{18}H_{34}O_2$	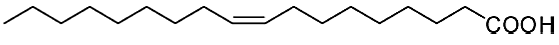
Linoleic	$C_{18}H_{32}O_2$	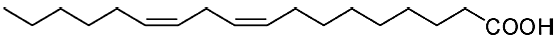
Linolenic	$C_{18}H_{30}O_2$	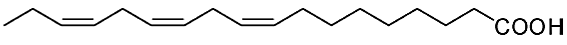
α-Eleostearic	$C_{18}H_{30}O_2$	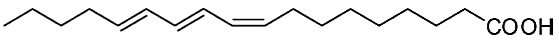
Ricinoleic	$C_{18}H_{34}O_3$	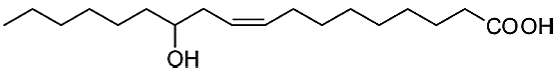
Vernolic	$C_{18}H_{32}O_3$	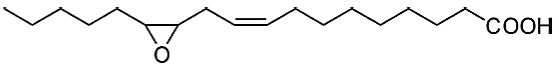

The Larock's research group in the Department of Chemistry at Iowa State University has prepared a variety of vegetable oil-based vinyl polymers utilizing the carbon-carbon double bonds in vegetable oils. Free radical polymerization, cationic polymerization, thermal polymerization, and ring-opening metathesis polymerization (ROMP) have been used to produce vegetable oil-based thermosets [9, 11-13]. Li et al. have prepared a range of thermosetting polymers by copolymerization of soybean oil with divinylbenzene (DVB) via cationic polymerization using boron trifluoride diethyl etherate (BFE) as the cationic initiator [14]. Three different types of soybean oil were used: regular soybean oil, low saturation soybean oil (a soybean oil that contains more carbon-carbon double bonds when comparing to regular soybean oil), and conjugated low saturation soybean oil. The reactivity of these three types of soybean oils is ranked as

follows: conjugated low saturation soybean oil > low saturation soybean oil > regular soybean oil. It was found that soybean oil was immiscible with the BFE cationic initiator while DVB was miscible with BFE [14]. Many white particulates were formed right after BFE initiator was added into the mixture containing soybean oil and DVB; however, the mixture was still in liquid state. The white particulates were found to be DVB polymers. This indicated a heterogeneous polymerization process, which yielded polymers with non-uniform density and poor mechanical properties. The heterogeneous reaction process was ascribed to the following two reasons [2]: (1) DVB has a much higher reactivity than soybean oil, leading to the formation of DVB polymers (the white particulate) right after BFE was added; (2) DVB was completely miscible with BFE while soybean oil was not miscible with BFE; as a result, BFE preferably reacted with DVB, forming many undesired white particulates. To overcome the heterogeneous reaction process, Norway fisher oil ethyl ester or soybean oil methyl ester was used to modify the BFE initiator because they are mutually soluble with soybean oil, BFE and DVB [2, 14].

The soybean oil-DVB system was further improved by the addition of monofunctional styrene [15]. The addition of styrene (ST) reduced the non-uniformity of and increased the mechanical properties, especially the toughness of the soybean oil-DVB system [16]. The reaction of copolymerization of soybean oil with ST and DVB is shown in Figure 1-2. A series of soybean oil-ST-DVB polymers have been produced with properties ranging from soft elastomers to rigid plastics. In the vegetable oils-ST-DVB system, DVB imparts rigidity, soybean oil imparts flexibility, and styrene can fine-tune the properties of the final materials by controlling the crosslink density.

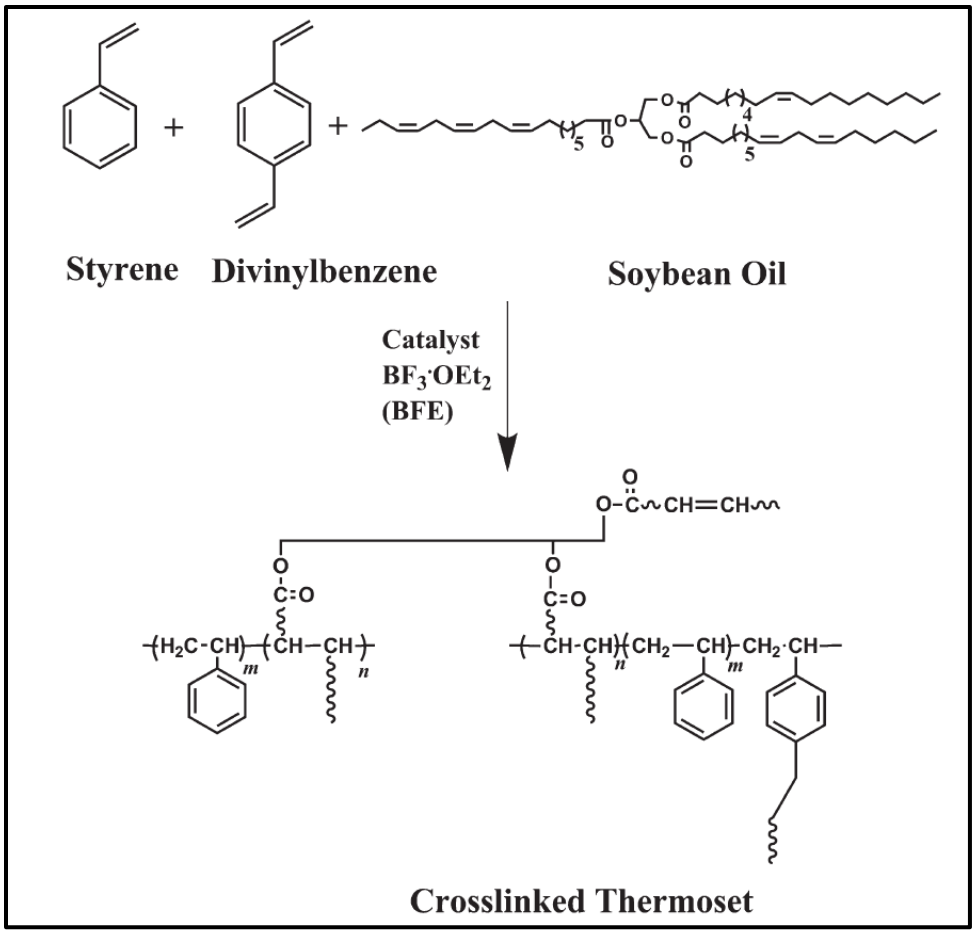

Figure 1-2: Chemical structures of styrene, divinylbenzene, soybean oil and their copolymers produced by cationic polymerization [17].

The vegetable oils-ST-DVB system polymerized by cationic initiator has been extensively studied with a variety of vegetable oils [11], including olive oil, peanut oil, sesame oil, canola oil, corn oil, soybean oil, grapeseed oil, sunflower oil, safflower oil, walnut oil, and linseed oil. Among these vegetable oils, the olive oil contains the least carbon-carbon double bonds while linseed oil contains the most. It was concluded that the use of vegetable oils containing more unsaturation sites leads to polymers with higher thermal stability and higher mechanical properties.

Rubbery materials have been produced from cationic copolymerization of conjugated soybean oil and dicyclopentadiene [18, 19]; however, the maximum engineering strain of this rubbery thermoset system is less than 300%, which is lower than most commercially available rubbers. Valverde et al. prepared rubbers from conjugated soybean oil cationically copolymerized with styrene and isoprene [20]. The resulting rubbers were also inferior to most commercially available rubbers in terms of elongation and strength.

In addition to cationic polymerization of the vegetable oil-ST-DVB resin system, other polymerization pathways were also explored. Conjugated linseed oil [21, 22] and tung oil [7] have been copolymerized with ST and DVB using the thermal polymerization method. However, the cure profile of this method is very energy intensive. The reactants were heated first at 85°C for 1h and then heated at 120°C for another 2 hours, followed by heating at 140°C for 24 h and 160°C for 24h. The cure schedule took more than 2 days. It was found that the tung oil-ST-DVB system possesses higher mechanical properties than the conjugated linseed oil-ST-DVB system. In addition, Soxhlet extraction data indicated that tung oil can be incorporated into the crosslinked network better than conjugated linseed oil. Metallic catalysts such as cobalt, calcium, and zirconium were also added to improve properties of vegetable oil-based polymers obtained by thermal polymerization [7]. It was found that these metallic catalysts can accelerate the thermal polymerization process and produce polymers with higher crosslink densities and higher mechanical properties [7].

Free radical polymerization of similar vegetable oil-based system was also performed. Henna et al. prepared conjugated linseed oil-acrylonitrile (AN) – DVB

polymer using 2,2′-azobisisobutyronitrile (AIBN) as the free radical initiator [23]. Dicyclopentadiene (DCPD) was also used as a crosslinker in free radical polymerization [24].

Ring-opening metathesis polymerization (ROMP) of vegetable oil has also been explored to produce thermosetting polymers. ROMP relies on the opening of strained rings, such as norbornene groups, to produce polymers. None of the vegetable oils contains norbornene groups in their natural forms. To produce ROMP-polymerizable vegetable oils, the vegetable oils must be chemically modified. Cargill Company (Chicago, IL) manufactures a commercially available DCPD-modified linseed oil with a trade name of Dilulin. An ROMP-based copolymer of Dilulin and DCPD has been polymerized by Grubb's catalyst [25]. Cui et.al used the Dilulin/DCPD copolymers as the matrix materials of glass fiber reinforced composites [26, 27]. It was also found that silane coupling agents can greatly increase the mechanical properties of the composites with Dilulin/DCPD as the matrix [26, 27].

The Wool's group from the University of Delaware is another active research group focusing on producing vegetable oils-based thermosets. To increase the reactivity of vegetable oils and the properties of vegetable oil-based polymer, Larock's group focused on conjugation of vegetable oils and copolymerizing them with petroleum-based copolymers, while Wool's group focused on transesterification and using anhydride to provide additional carbon-carbon double bonds. Can et al. produced thermosetting polymers by free radically polymerizing soybean oil monoglyceride maleates [28]. To prepared soybean oil monoglyceride (SOMG), glycerol was first added into soybean oil, and the reaction mixture was then heated up to 220°C. Transesterification will occur

between the soybean oil and glycerol, and SOMG was produced. Maleic anhydride was then added into the SOMG to produce SOMG maleates, and SOMG maleates were copolymerized with styrene to produce thermosetting polymers. The above reaction process is shown in Figure 1-3. Similar synthesis pathway has also been performed on linseed oil [29]. Since the carbon-carbon double bonds on soybean oil and linseed oil are not conjugated, the double bonds on the fatty acid chains of SOMG cannot be incorporated into the polymer network; thus the fatty acid chains will have plasticizing effect on the resulting polymer [9]. To further increase the mechanical properties of SOMG-ST copolymer, bisphenol A and neopentyl glycol were added into SOMG [30]. The resulting thermosets possess a tensile modulus value of 1.49 GPa and a tensile strength around 30 MPa [30].

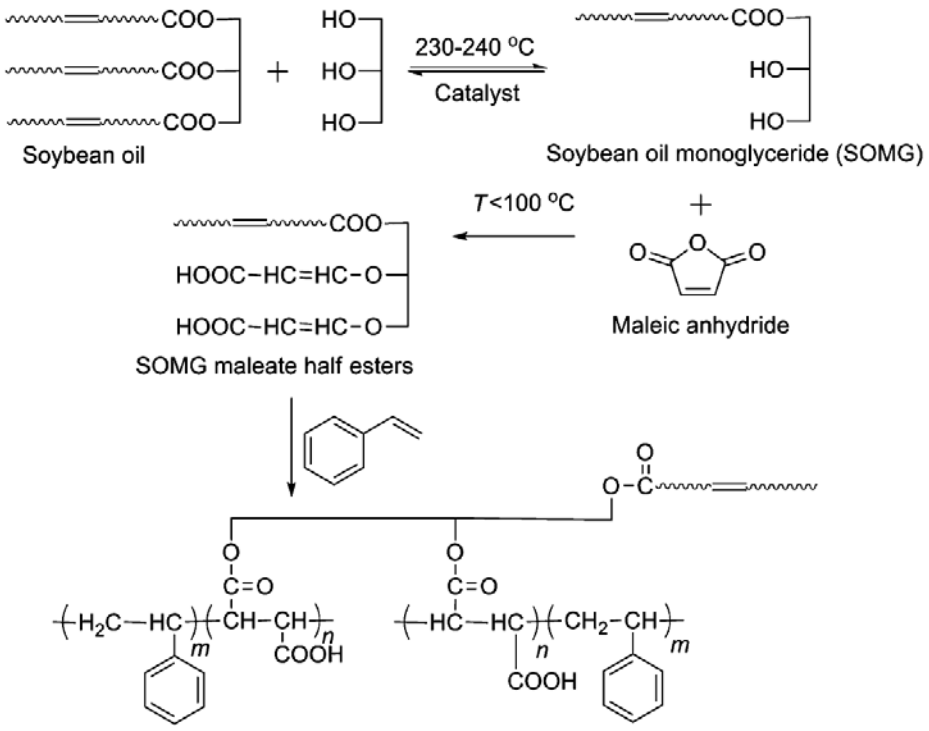

Figure 1-3: Synthesis of soybean oil monoglyceride maleates and copolymerization with styrene [28].

Can et al. prepared castor oil monoglyceride (COMG) using the same technique as that of preparation of SOMG [31, 32]. Since castor oil contains hydroxyl groups on the fatty acid chain, maleic anhydride can attack the hydroxyl group, providing more reactive unsaturation sites on COMG. Comparison of mechanical properties between polymers prepared from SOMG-maleate and COMG-maleate showed that COMG is a better candidate than SOMG to produce polymers with high strength and modulus [32].

Acrylated epoxidized soybean oil (AESO) is another common form of soybean oil. It is synthesized by first reacting soybean oil hydrogen peroxide and formic acid to produce epoxidized soybean oil (ESO). ESO was then reacted with acrylic acid to produce AESO. Compared to regular soybean oil, the carbon-carbon doubles bonds originally on the fatty acid chains are transformed into acrylate groups; and the double bonds on the acrylate groups are much more reactive than the double bonds on the regular soybean oil. AESO can undergo free radical polymerization by itself since the acrylate groups are very reactive. Since AESO contains hydroxyl groups, it can be further modified by anhydride that contains carbon-carbon doubles bonds to introduce more unsaturation site. Maleic anhydride and methacrylic anhydride have been used to modify AESO to increase the unsaturation sites in AESO [33, 34]. Another approach to modify AESO is by using diacid or dianhydrides to oligomerize AESO, which will increase the entanglement between the triglyceride chains as well as introducing stiff cyclic rings into the structure, thus increasing the Young's modulus and strength of the obtained thermoset [5]. Cyclohexane dicarboxylic anhydride and phthalic anhydride have been used for this purpose [5, 35].

This introduction only covers some of the vegetable oils-based thermosetting polymers that utilize the carbon-carbon double bonds as crosslinking sites. In addition to the discussed vinyl thermosetting polymers, vegetable oil-based polyamides, polyurethanes, poly(ester amide)s, polyesters, and epoxies have also been synthesized [36, 37]. A variety of vegetable oil-based polymer composites and nanocomposites were extensively studied [38-40]. Polymers based or other biorenewable resources, such as polysaccharides, lignin, sugars, terpenes, rosins, polycarboxylic acids, furans, and glycerol have also been prepared [41].

1.3 Objectives

The aim of my research is to develop various biorenewable polymers for different applications. The goal of the study presented in Chapter 2 is to develop a vegetable oil-based thermoset system that will be used in pultrusion process. The aim of the study presented in Chapter 3 is to develop a lost-cost biocomposites with biorenewable matrix and biorenewable fillers for bioplastic cropping container systems. After a suitable candidate material that can meet the need of the project sponsors was found, various material characterization techniques were used to understand the newly developed materials. Dynamic mechanical analysis (DMA), differential scanning calorimetry (DSC), thermogravimetric analysis (TGA), rheology, mechanical testing, and scanning electron microscopy (SEM) were used.

1.4 References

[1] Williams CK, Hillmyer MA. Polymers from renewable resources: A perspective for a special issue of polymer reviews. Polym Rev. 2008;48(1):1-10.

[2] Li FK, Larock RC. New soybean oil-styrene-divinylbenzene thermosetting copolymers. I. Synthesis and characterization. J Appl Polym Sci. 2001;80(4):658-70.

[3] Larock RC, Dong XY, Chung S, Reddy CK, Ehlers LE. Preparation of conjugated soybean oil and other natural oils and fatty acids by homogeneous transition metal catalysis. J Am Oil Chem Soc. 2001;78(5):447-53.

[4] Li FK, Larock RC. New soybean oil-styrene-divinylbenzene thermosetting copolymers. VI. Time-temperature-transformation cure diagram and the effect of curing conditions on the thermoset properties. Polym Int. 2003;52(1):126-32.

[5] Khot SN, Lascala JJ, Can E, Morye SS, Williams GI, Palmese GR, et al. Development and application of triglyceride-based polymers and composites. J Appl Polym Sci. 2001;82(3):703-23.

[6] Ma QQ, Liu XQ, Zhang RY, Zhu J, Jiang YH. Synthesis and properties of full bio-based thermosetting resins from rosin acid and soybean oil: the role of rosin acid derivatives. Green Chem. 2013;15(5):1300-10.

[7] Li FK, Larock RC. Synthesis, structure and properties of new tung oil-styrene-divinylbenzene copolymers prepared by thermal polymerization. Biomacromolecules. 2003;4(4):1018-25.

[8] Belgacem MN, Gandini A. Monomers, polymers and composites from renewable resources. 1st ed. Amsterdam ; Boston: Elsevier; 2008.

[9] Xia Y, Larock RC. Vegetable oil-based polymeric materials: synthesis, properties, and applications. Green Chem. 2010;12(11):1893-909.

[10] Stevens CV, Verhé R. Renewable bioresources : scope and modification for non-food applications. Chichester, West Sussex, England ; Hoboken, NJ: Wiley; 2004.

[11] Andjelkovic DD, Valverde M, Henna P, Li FK, Larock RC. Novel thermosets prepared by cationic copolymerization of various vegetable oils - synthesis and their structure-property relationships. Polymer. 2005;46(23):9674-85.

[12] Lu YS, Larock RC. Novel Polymeric Materials from Vegetable Oils and Vinyl Monomers: Preparation, Properties, and Applications. Chemsuschem. 2009;2(2):136-47.

[13] Sharma V, Kundu PP. Addition polymers from natural oils - A review. Prog Polym Sci. 2006;31(11):983-1008.

[14] Li F, Hanson MV, Larock RC. Soybean oil-divinylbenzene thermosetting polymers: synthesis, structure, properties and their relationships. Polymer. 2001;42(4):1567-79.

[15] Li FK, Larock RC. New soybean oil-styrene-divinylbenzene thermosetting copolymers. II. Dynamic mechanical properties. J Polym Sci Pol Phys. 2000;38(21):2721-38.

[16] Li FK, Larock RC. New soybean oil-styrene-divinylbenzene thermosetting copolymers. III. Tensile stress-strain behavior. J Polym Sci Pol Phys. 2001;39(1):60-77.

[17] Badrinarayanan P, Lu YS, Larock RC, Kessler MR. Cure Characterization of Soybean Oil-Styrene-Divinylbenzene Thermosetting Copolymers. J Appl Polym Sci. 2009;113(2):1042-9.

[18] Andjelkovic DD, Larock RC. Novel rubbers from cationic copolymerization of soybean oils and dicyclopentadiene. 1. Synthesis and characterization. Biomacromolecules. 2006;7(3):927-36.

[19] Andjelkovic DD, Lu YS, Kessler MR, Larock RC. Novel Rubbers from the Cationic Copolymerization of Soybean Oils and Dicyclopentadiene, 2-Mechanical and Damping Properties. Macromol Mater Eng. 2009;294(8):472-83.

[20] Valverde M, Yoon S, Bhuyan S, Larock RC, Kessler MR, Sundararajan S. Rubbers Based on Conjugated Soybean Oil: Synthesis and Characterization. Macromol Mater Eng. 2011;296(5):444-54.

[21] Kundu PP, Larock RC. Novel conjugated linseed oil-styrene-divinylbenzene copolymers prepared by thermal polymerization. 1. Effect of monomer concentration on the structure and properties. Biomacromolecules. 2005;6(2):797-806.

[22] Sharma V, Banait JS, Larock RC, Kundu PP. Morphological and Thermal Characterization of Linseed-Oil Based Polymers from Cationic and Thermal Polymerization. J Polym Environ. 2010;18(3):235-42.

[23] Henna PH, Andjelkovic DD, Kundu PP, Larock RC. Biobased thermosets from the free-radical copolymerization of conjugated linseed oil. J Appl Polym Sci. 2007;104(2):979-85.

[24] Valverde M, Andjelkovic D, Kundu PP, Larock RC. Conjugated low-saturation soybean oil thermosets: Free-radical copolymerization with dicyclopentadiene and divinylbenzene. J Appl Polym Sci. 2008;107(1):423-30.

[25] Henna P, Larock RC. Novel Thermosets Obtained by the Ring-Opening Metathesis Polymerization of a Functionalized Vegetable Oil and Dicyclopentadiene. J Appl Polym Sci. 2009;112(3):1788-97.

[26] Cui HY, Kessler MR. Pultruded glass fiber/bio-based polymer: Interface tailoring with silane coupling agent. Compos Part a-Appl S. 2014;65:83-90.

[27] Cui HY, Kessler MR. Glass fiber reinforced ROMP-based bio-renewable polymers: Enhancement of the interface with silane coupling agents. Compos Sci Technol. 2012;72(11):1264-72.

[28] Can E, Kusefoglu S, Wool RP. Rigid, thermosetting liquid molding resins from renewable resources. I. Synthesis and polymerization of soy oil monoglyceride maleates. J Appl Polym Sci. 2001;81(1):69-77.

[29] Mosiewicki M, Aranguren MI, Borrajo J. Mechanical properties of linseed oil monoglyceride maleate/styrene copolymers. J Appl Polym Sci. 2005;97(3):825-36.

[30] Can E, Kusefoglu S, Wool RP. Rigid thermosetting liquid molding resins from renewable resources. II. Copolymers of soybean oil monoglyceride maleates with neopentyl glycol and bisphenol A maleates. J Appl Polym Sci. 2002;83(5):972-80.

[31] Can E, Wool RP, Kusefoglu S. Soybean and castor oil based monomers: Synthesis and copolymerization with styrene. J Appl Polym Sci. 2006;102(3):2433-47.

[32] Can E, Wool RP, Kusefoglu S. Soybean- and castor-oil-based thermosetting polymers: mechanical properties. J Appl Polym Sci. 2006;102(2):1497-504.

[33] Adekunle K, Akesson D, Skrifvars M. Synthesis of Reactive Soybean Oils for Use as a Biobased Thermoset Resins in Structural Natural Fiber Composites. J Appl Polym Sci. 2010;115(6):3137-45.

[34] Lu J, Hong CK, Wool RP. Bio-based nanocomposites from functionalized plant oils and layered silicate. J Polym Sci Pol Phys. 2004;42(8):1441-50.

[35] Zhan MJ, Wool RP. Biobased Composite Resins Design for Electronic Materials. J Appl Polym Sci. 2010;118(6):3274-83.

[36] Karak N. Vegetable oil-based polymers properties, processing and applications. Cambridge, UK ; Philadelphia: Woodhead Publishing; 2012.

[37] Mulhaupt R. Green Polymer Chemistry and Bio-based Plastics: Dreams and Reality. Macromol Chem Phys. 2013;214(2):159-74.

[38] Lligadas G, Ronda JC, Galia M, Cadiz V. Renewable polymeric materials from vegetable oils: a perspective. Mater Today. 2013;16(9):337-43.

[39] Mustapha SNH, Rahmat AR, Arsad A. Bio-based thermoset nanocomposite derived from vegetable oil: a short review. Rev Chem Eng. 2014;30(2):167-82.

[40] Mohanty AK, Misra M, Drzal LT. Natural fibers, biopolymers, and biocomposites. Boca Raton, FL: Taylor & Francis; 2005.

[41] Gandini A. The irruption of polymers from renewable resources on the scene of macromolecular science and technology. Green Chem. 2011;13(5):1061-83.

CHAPTER 2 : BIO-BASED THERMOSETTING POLYMER BASED ON SOYBEAN OIL AND EUGENOL

A paper to be submitted to the European Polymer Journal

Kunwei Liu[a], Samy A. Madbouly[ab], Michael R. Kessler[c],

[a] Department of Materials Science and Engineering, Iowa State University, Ames, IA, USA

[b] Department of Chemistry, Faculty of Science, Cairo University, Orman-Giza, Egypt

[c]School of Mechanical and Materials Engineering, Washington State University, Pullman, WA, USA

2.1 Abstract

A novel biorenewable thermoset based on acrylated epoxidized soybean oil (AESO) and methacrylated eugenol (ME) was prepared via free radical polymerization. The chemical compositions of the monomers were investigated using proton nuclear magnetic resonance (1H NMR) technique. The properties of this resin system were investigated using small amplitude oscillatory shear flow rheology, dynamical mechanical analysis (DMA), thermogravimetric analysis (TGA), and compression testing. Soxhlet extraction was also performed on the cured thermoset to determine the percentage of monomers that are incorporated into the crosslink network. In addition, the gelation time of this resin at different curing temperature was also monitored using a rheometer. The Soxhlet extraction data indicated that more than 95% of the monomers were incorporated into the crosslink network. Gelation time study showed that this resin system can become a solid within 10 min. This resin system possesses high strength and

modulus, and it is thermal stable up to 300°C. This high biorenewable content resin system possesses good mechanical properties, high thermal stability, and fast curing speed, making it a suitable matrix resin for the pultrusion process and other composite manufacturing processes.

2.2 Introduction

In recent years, polymeric materials derived from biorenewable resources have attracted a lot of attention due to the shortage and high price of petroleum and the increase in environmental concerns. Currently, almost all commercially available polymers are derived from non-sustainable petroleum resources. About 7% of oil and gas are used to produce plastic [1]. A wide range of biorenewable polymeric materials have been developed that utilize biorenewable resources such as sugars, polysaccharides, lignins, plant oils, pine resin derivatives, and furans [2].

Vegetable oils are one of the most abundant biorenewable materials. Their inherent biodegradability and low toxicity make them a promising starting material for polymer synthesis. Vegetable oils are composed of triglyceride molecules. Triglycerides consist of three fatty acid chains combined with glycerol through ester linkage. The length of fatty acid ranges from 8-22 carbon, and some of them have chemical functionalities such as hydroxyl groups, epoxide groups, and unsaturation (carbon-carbon double bond) [3]. Recently, there are many research activities focusing on using vegetable oil as partial replacement of petroleum components in plastic. Vegetable oils such as soybean oil [4-6], linseed oil [7-9], corn oil [10], and tung oil [11-13] contain unsaturation sites (carbon-carbon double bonds) and have been copolymerized with petroleum-based chemicals, such as styrene (ST), divinylbenzene (DVB),

dicyclopentadiene (DCPD), and acrylonitrile using cationic, free radical or thermal polymerization. The properties of the resulting thermosetting polymers range from rigid plastics to soft and flexible rubbers. However, soybean oil, corn oil, and linseed oil do not contain conjugated double bonds in their triglyceride chains, thus making them difficult to be incorporated into the crosslinked thermoset network. Conjugation of vegetable oil can be accomplished using catalysts containing rhodium or ruthenium [14]. On the other hand, epoxidation can be performed on vegetable oil to turn the carbon-carbon double bonds into oxirane rings [15, 16]. The epoxidized vegetable oils (EVO) can be blended into commercially available epoxy systems to yield a new class of epoxy. Epoxidized vegetable oils have been blended with commercially available epoxy systems such as Bisphenol A diglycidyl ether (DGEBA) and Di-Glycidyl Ether of Bisphenol F (DGEBF) [17, 18]. It was found that the storage modulus at room temperature, the glass transition temperature, and the crosslink density of the epoxy blend decreased with increasing content of EVO, while fracture toughness and flexural modulus were increased with increasing amount of EVO [17-19]. The epoxide rings of EVO can be ring-opened by alcohols [20] or acids [21, 22] to introduce other functionalities. After the epoxide rings had been opened, hydroxyl groups were introduced, and polyurethanes with a wide range of properties can be produced by the reactions between hydroxyl groups and diisocyanates [23]. EVO can also be ring-opened to produce molecules with acrylates to increase the reactivity of vegetable oils.

Acrylate epoxidized soybean oil (AESO) is produced by reacting epoxidized soybean oil with acrylic acid [24], and the steps of synthesizing AESO is shown in Figure 2-1. AESO is commercially available under the trade name Ebecryl 860, and it can be

polymerized using free radical initiators [25, 26]. Due to the high viscosity of AESO, it has been copolymerized with styrene to increase its processiblity [26, 27]. AESO has also been combined with hemp fibers [25], cellulose fibers [28], pyrolyzed chicken feather [29], and montmorillonite clay [30] to produce composites with high renewable content. In addition, it has been proposed that AESO-based resins can be used in electronics [31, 32] and coating applications [33].

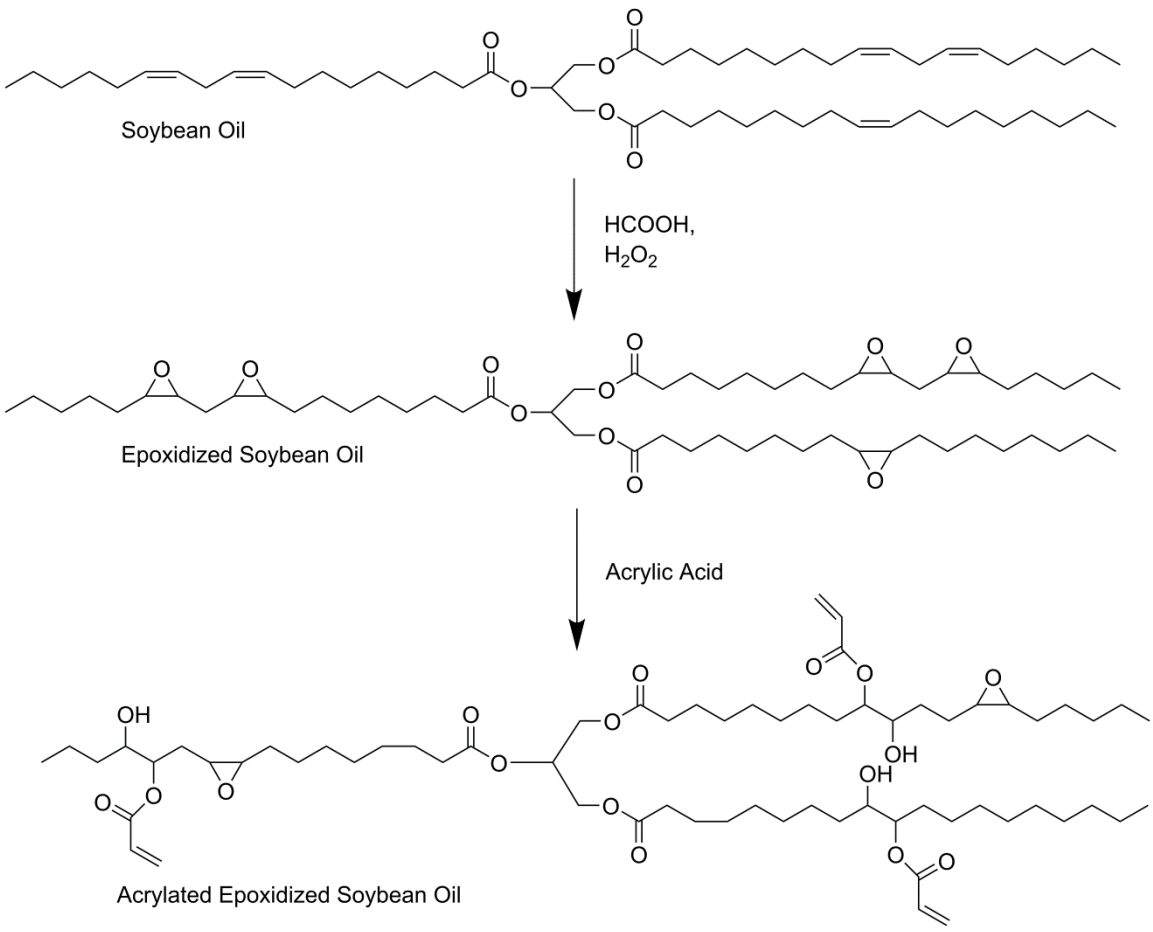

Figure 2-1: Synthesis of acrylated epoxidized soybean oil (AESO).

Eugenol is an aromatic compound found in plants such as clove, cinnamon, basil, and nutmeg. It is considered a safe additive to food and has been used as a flavoring

agent in cosmetic and food products [34]. The combination of eugenol and zinc oxide has been widely used in the dental industry as a cement material [35]. Eugenol also has antibacterial property, and it has been incorporated into polypropylene to produce antibacterial plastics [36]. Qin et. al has attached epoxy groups onto eugenol to produce a biorenewable epoxy system [37]. Polyacetylene based on eugenol and propargyl chloride has also been synthesized, with molecular weight above M_n = 30000 g/mol [38]. High-performance bismaleimide resin has also been synthesized utilizing eugenol and succinic acid [39]. On the other hand, even though nowadays eugenol is extracted from clove, studies have shown that eugenol can potentially be obtained from pyrolysis [40, 41] or depolymerization [42] of lignin. Because of the low cost and abundance of lignin, the price of eugenol can be dramatically decreased if an economical pathway of obtaining eugenol from lignin is developed.

Pultrusion is a low-cost, highly automatic manufacturing process to produce fiber reinforced composites with constant cross-section profile [43]. In the pultrusion process, fibers are impregnated with the resin, and the fibers are then pulled by a motor through a heated die with desired geometry. In the heated die, the resin (the matrix of the composites) becomes cured and fiber reinforced composites are produced. There are many studies focusing on incorporating biorenewable fibers, such as jute, hemp, and kenaf fibers into a petroleum based matrix [44-46]; however, there are few studies focusing on developing a biorenewable matrix materials suitable for the pultrusion process. Cui et al. prepared glass fiber reinforced composites using dicyclopentadiene and norbornene-modified linseed oil copolymerized by ring-opening metathesis [47]. Badrinarayanan studied the cure kinetic of soybean oil-ST-DVB copolymer system and

found that this system is suitable for pultrusion due to its fast curing speed [48]. Chandrashekhara et al. used the pultrusion process on the blend of epoxidized allyl soyate (a mixture of epoxidized fatty acid ester) and Epon 9500 (a commercially available epoxy resin designed for pultrusion) to produce glass fiber reinforced composites [49]. It was found that incorporation of 10 wt% to 20 wt% of epoxidized allyl soyate into epoxy yielded a material with a toughness that is much higher than pure epoxy [49]. However, the above resin systems consist of more than 50% of non-biorenewable contents; as a result, the aim of this work is to develop a vegetable oil-based thermosetting resin with high biorenewable content that is suitable for the pultrusion process.

2.3 Experiment Details

2.3.1 Materials

Eugenol (98%), acrylated epoxidized soybean oil, methacrylic anhydride (94%, containing 2000 ppm Topanol A inhibitor), 4-dimethylaminopyridine (DMAP), and benzoyl peroxide (BPO) free radical initiator were purchased from Sigma Aldrich (Milwaukee, WI). Methylene chloride (CH_2Cl_2), sodium bicarbonate, sodium hydroxide (NaOH), hydrochloric acid (HCL), magnesium sulfate (anhydrous) ($MgSO_4$) were obtained from Fisher Scientific. Deuterated chloroform for nuclear magnetic resonance (NMR) analysis was purchased from Cambridge Isotope Laboratories, Inc. All chemicals were used as received without further purification.

2.3.2 Synthesis of methacrylated eugenol

The methacrylation of eugenol is performed as described in literature [50], and the synthesis route is shown in Figure 2-2. 100 g of eugenol (0.61 mol) and 2.51 g of

DMAP (2 mol% of methacrylic anhydride) were added into a 500 ml round-bottom flask equipped with a magnetic stir bar and a nitrogen gas inlet. After the flask had been purged with nitrogen gas for at least an hour to remove the oxygen and moisture, 98.7g methacrylic anhydride (105 mol% of eugenol) was added into the flask. For the first three hours of the reaction, the flask was placed at room temperature. The flask was then heated to 45 °C under a nitrogen atmosphere and kept at this temperature for at least 24 hours. The reaction mixture was then transferred to a 2000 mL Erlenmeyer flask, and 500 mL of CH_2Cl_2 was added to the reaction mixture. To remove the methacrylic acid byproduct and unreacted methacrylic anhydride, the organic phase was washed with 1L of saturated sodium bicarbonate aqueous solution, 1.0 M NaOH aqueous solution, 0.5 M NaOH aqueous solution, 1.0 M of hydrochloric acid, and water. Each wash was repeated at least twice. After the above washing steps, the mixture was dried with anhydrous $MgSO_4$ powder overnight. The mixture was then filtered to remove solid $MgSO_4$, and was followed by concentration under reduced pressure to remove the CH_2Cl_2.

2.3.3 Free radical polymerization of AESO/ME copolymers

Pre-weighed amounts of AESO and ME were added to a vial, followed by the addition of 2 wt% of BPO free radical initiator. The reaction mixture was stirred vigorously using a Kurabo MAZERUSTAR (Tokyo, Japan) planetary mixer until the mixture became homogeneous and all the BPO free radical initiator was dissolved. The homogeneous mixture was then degassed under reduced pressure and poured into a silicon mold. The resin was cured for 2 hours at 90°C and 4 hours at 160°C. The samples were then post-cured at 200°C for 2 hours. The heating rate for the above-stated cure schedule was set to be 1°C per minute. The following system of nomenclature has been

adopted for simplicity: AESO20 corresponds to a polymer sample prepared from 20 wt% AESO, 78 wt% ME, and 2 wt% BPO initiator.

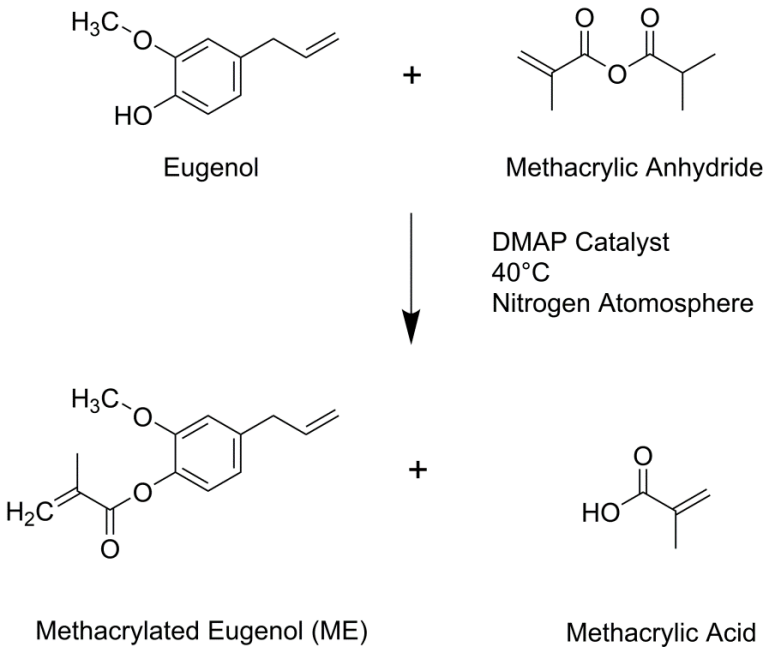

Figure 2-2: Synthesis of methacrylated eugenol.

2.3.4 Material Characterizations

2g of the bulk polymer sample was extracted with 400 mL of refluxing CH_2Cl_2 in a Soxhlet extractor for 24 hours. After extraction, the insoluble portion of the sample was separated from the CH_2Cl_2 solvent and was dried under vacuum at 70°C for at least 24 hours before weighing.

1H-NMR of the synthesized ME was performed in deuterated chloroform using a Varian Unity spectrometer (Varian Associates, Palo Alto, CA) at 400 MHz. The data was obtained by averaging 32 scans.

Dynamic mechanical analysis (DMA) was carried out using a TA Q800 dynamic mechanical analyzer in tension mode. Rectangular specimen with dimensions approximating 1.0 mm thickness, 4.0 mm width, and 8.5 mm length were heated from -100°C to 200°C with a heating rate of 3°C/min. All DMA measurements were performed under a frequency of 1 Hz and displacement amplitude of 5 μm.

The thermal stability of the obtained copolymers was studied using a TA Q50 thermogravimetric analyzer. Approximately 5-8 mg of sample was heated from room temperature to 800°C in a nitrogen atmosphere with a heating rate of 20°C/ minute.

The gelation process of the AESO/ME copolymerization was studied using TA AR2000ex rheometer using parallel plates with 25 mm diameter. Time sweeps at a constant shear frequency of 10 rad/s at 70°C, 80°C, and 90°C were performed on the AESO/ME mixture containing 2 wt% BPO initiator. The time when the storage modulus (G') and the loss modulus (G") intercepted is considered the gelation time. In addition, the viscosity of the AESO/ME mixture was also measured using a steady state procedure with shear rates increasing from 10 s^{-1} to 200 s^{-1}. The measurement was conducted at 25°C.

Compression testing of the AESO/ME copolymers was performed according to ASTM standard D695-10 using an Instron 5569 load frame. A specimen size of 12.7mm by 12.7mm by 25.4 mm was used. The crosshead speed was set at 1.3 mm/min. A minimum of five samples were tested for each composition.

2.4 Result and Discussion

2.4.1 Synthesis of AESO/ME copolymers

A thermosetting resin for pultrusion process must possess the following characteristics: low to medium viscosity, fasting curing process, and high rigidity after cure. Unsaturated polyesters are the most commonly used resins for pultrusion application, and styrene is always added to reduce the viscosity of the unsaturated polyesters. Eugenol is a low viscosity liquid at room temperature, and it also has an aromatic ring and a double bond; as a result, the molecular structure of eugenol is similar to styrene. In addition, eugenol is more environmental friendly when compared to styrene because eugenol is a bio-based chemical with low toxicity. However, unlike styrene, eugenol will not polymerize by itself by free radical polymerization because phenol derivatives are chain breaking radical scavengers, which means that the free radicals generated by free radical initiators are trapped in the phenolic hydroxyl group in eugenol [51]. In fact, eugenol has been used as a free radical polymerization retarder [52]. Adding the methacrylate functional group onto the eugenol allows it to become a polymerizable monomer. Methacryalted eugenol is a very reactive product. By adding 2 wt% BPO free radical initiator into ME and heating the reaction mixture at 110°C, a rigid thermoset was produced in less than two minutes. The fast reaction process of ME, combined with its low viscosity and rigid aromatic structure makes ME a good candidate material for pultrusion application.

Figure 2-3 depicts the crosslinking reaction between AESO and ME. ME contains two types of double bonds: the double bonds on the acrylate groups and the allylic double bonds. These two types of double bond can both participate in the crosslinking reaction

[53]. On the other hand, AESO has only one type of double bonds. AESO and ME are completely miscible to each other, and the cured samples were homogeneous and transparent with a color similar to that of soybean oil. No separation was observed on all cured samples.

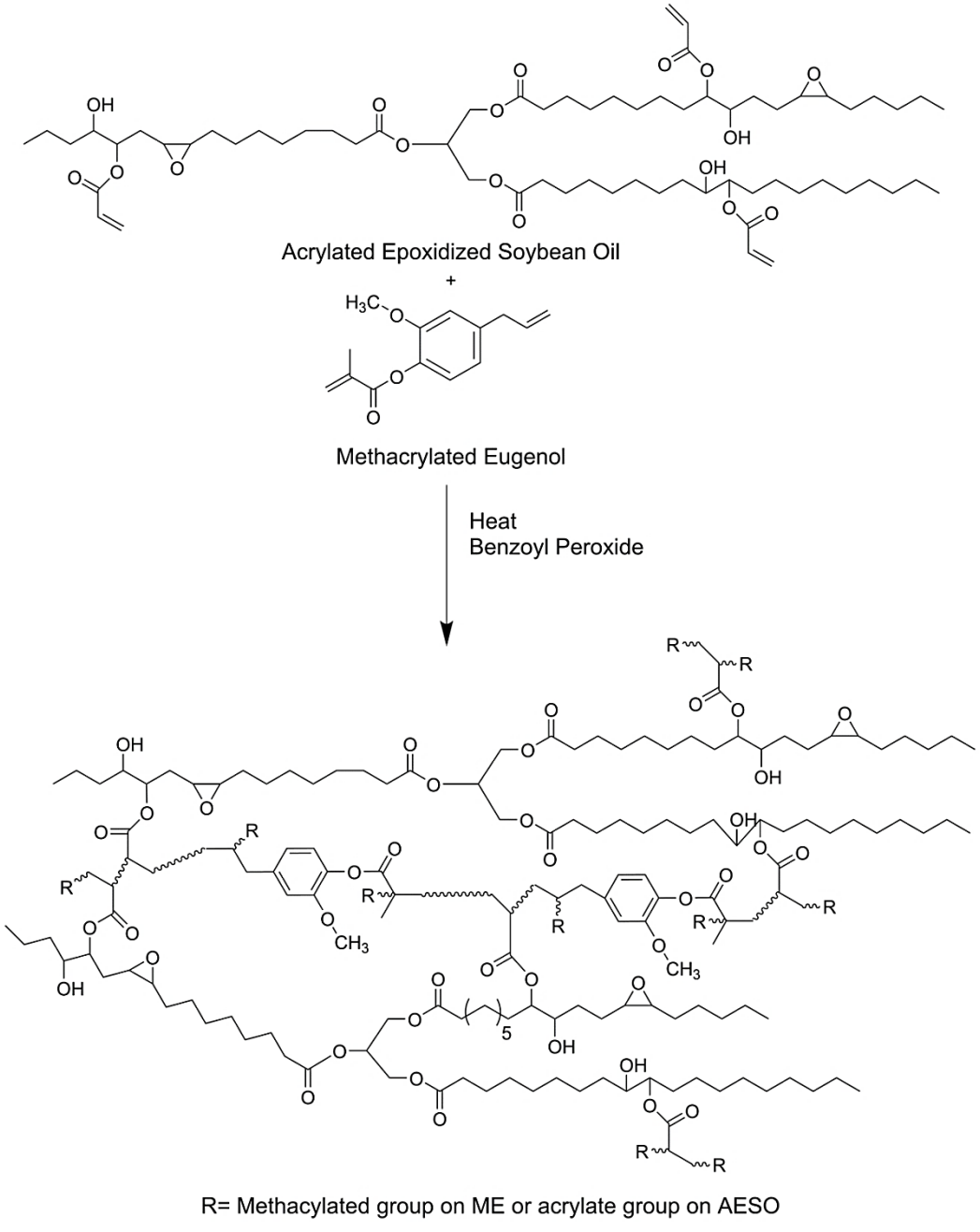

Figure 2-3: The crosslinking reaction between AESO and ME.

2.4.2 NMR

The ^{1}H NMR spectra of as-receive eugenol and methacrylated eugenol are shown in Figure 2-4 and Figure 2-5, respectively. In the NMR spectra of the as-received eugenol, the peaks at 6.6 – 7.0 ppm originate from the hydrogen atoms bonding to the aromatic rings. The peaks in the range of 4.75 – 5.2 ppm represent the two hydrogen atoms connecting to the terminal side allylic double bond of eugenol. The multiplet in the range of 5.8 – 6.0 ppm comes from the hydrogen on the secondary carbon of the allylic double bond.

After the methacrylation reaction, the aromatic hydroxyl group was replaced by methacrylate group. This is evident by the presence of peaks between 6.2 ppm and 6.4 ppm, which comes from the proton from the terminal carbon of the methacrylate group. The additional peak on 2.1 ppm represents the proton found on the secondary carbon of the methacrylated group, which is not seen on the spectrum of as-received eugenol. However, there are trace amounts of impurities on the ME. The impurities come from the topanol A, which is a photodegradation inhibitor presented in the as-received methacrylic anhydride. The trace amount of impurities does not inhibit the polymerization of ME. The synthesized ME can be further purified using silica gel.

A ^{1}H NMR spectrum of AESO is shown in Figure 2-6. The three peaks in the range of 5.7 – 6.6 ppm represent the three hydrogen atoms of the acrylate function groups. The peak between 0.7 – 1 ppm comes from the hydrogen atoms attaching to the terminal carbon of the triglyceride molecules. The triplet peak between 2.1 to 2.4 ppm is related to the hydrogen atom at the alpha position of the carbonyl groups. The peaks between 4.0 to 4.5 ppm come from the protons on the primary carbon group near the

center of the triglyceride. The number of acrylate groups per triglyceride molecule can be calculated by dividing the area under the acrylate peaks (5.7 – 6.6 ppm) by the area under the peak terminal carbon (0.7 – 1 ppm) and by multiplying the quotient by three. It is found that there are 3.4 acrylate groups per triglyceride molecule.

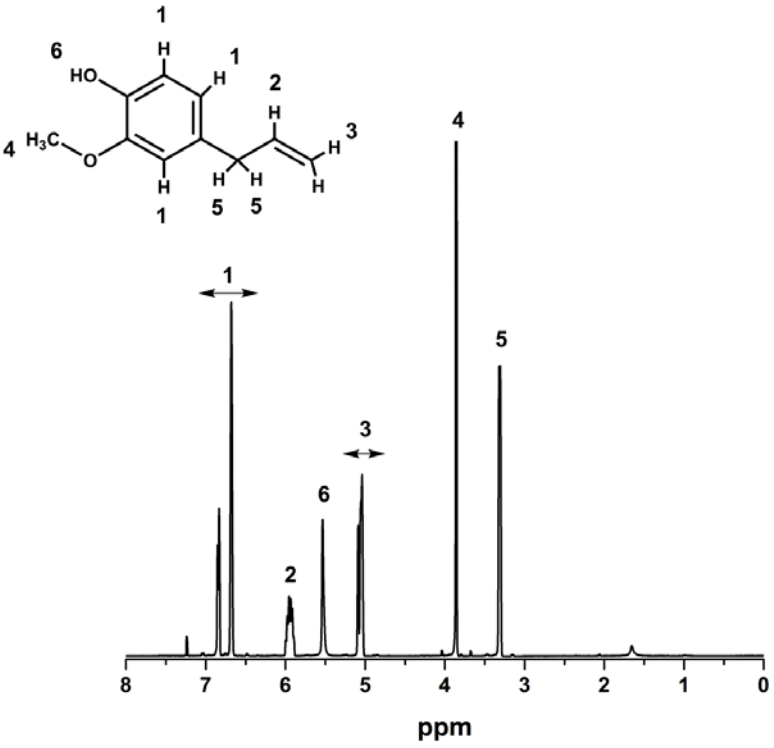

Figure 2-4: ^{1}H NMR spectrum of as-received eugenol.

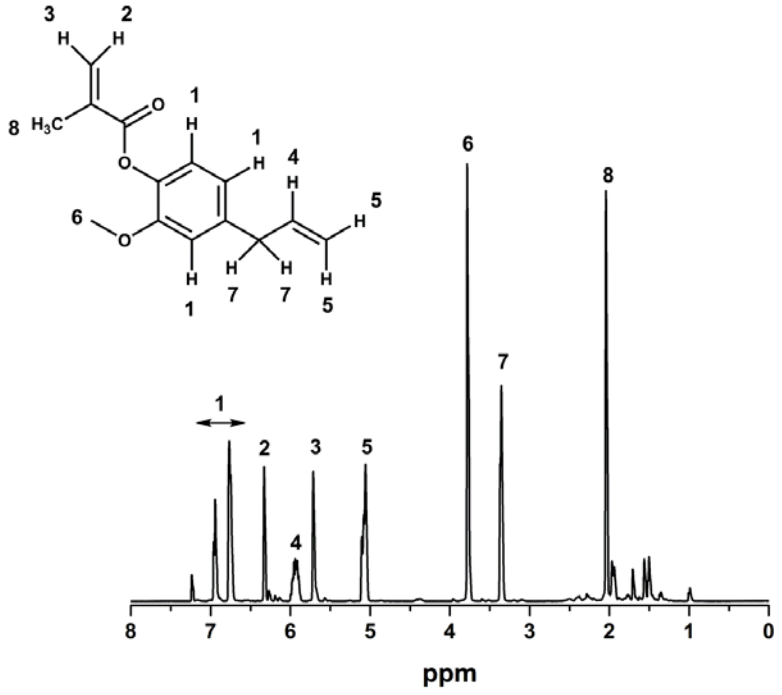

Figure 2-5: ^{1}H NMR spectrum of methacrylated eugenol.

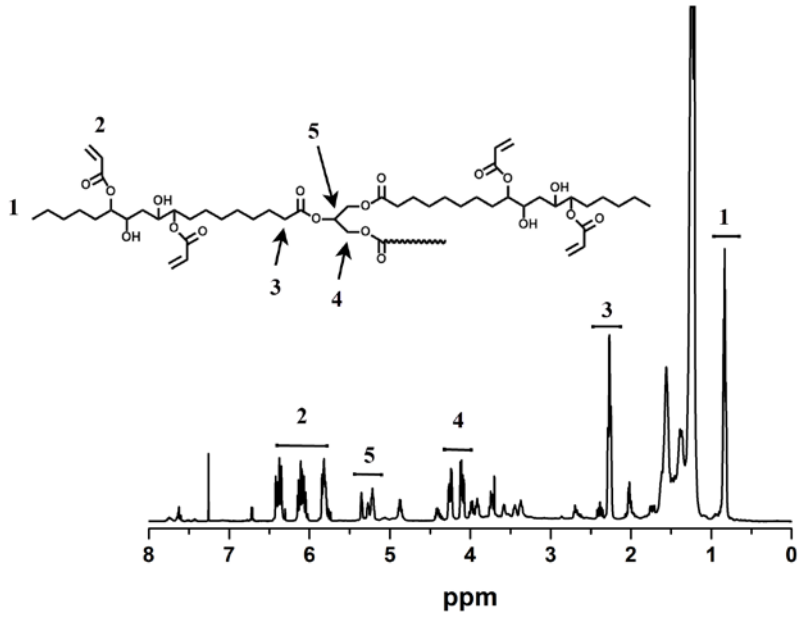

Figure 2-6: ^{1}H NMR spectrum of acrylated epoxidized soybean oil.

2.4.3 Soxhlet extraction

Soxhlet extraction was performed to measure the percentage of monomers incorporated in the thermoset network, and the data are summarized in Table 2-1. The soluble portion extracted from the bulk polymer consists of substances that are unreacted monomers or low molecular weight polymers. The insoluble portion of the polymer varied from 97.7% to 99.3%, indicating that the majority of AESO and ME have participated in the crosslinking reaction. The crosslinked portion in the AESO/ME system is found to be much higher than the conjugated vegetable oil-styrene-divinylbenzene system developed by Li et al. [4].

Table 2-1: Soxhlet extraction data for all copolymers.

Polymer Composition	Soluble (%)	Insoluble (%)
AESO0-ME98	99.3	0.7
AESO10-ME88	97.7	2.3
AESO20-ME78	97.7	2.3
AESO30-ME68	98.2	1.8
AESO40-ME58	97.9	2.1

2.4.4 Rheological properties

A rheometer was used to monitor the gelation time at 70°C, 80°C and 90°C. The gelation time can be found that the intercept of storage modulus and loss modulus [54]. The value of the gelation time is found to be dependent on the chemical composition of the AESO/ME copolymer. Figure 2-7 shows a plot of gelation time vs. AESO content at different curing temperatures. At a given curing temperature, the gelation time decreases as the AESO content increases, and this is ascribed to the fact that acrylate functional

groups generally have higher reactivity than methacrylate functional groups. As the AESO content in the mixture increases, there are more acrylate functional groups (from AESO) and less methacrylate functional groups (from ME) in the mixture; as a result, the crosslinking reaction proceeded faster with higher AESO content. For a curing temperature of 90°C, the gelation time ranges from 4.7 min (40 wt% AESO) to 6.7 min (0 wt% AESO). At this curing temperature, the mixture can become a solid gel within 10 min. The fast gelation speed of the AESO/ME system indicates that this system is a suitable candidate for pultrusion. An even shorter gelation time can be achieved by curing this resin at a temperature higher than 90°C; however, at such a high temperature, the mixture cured almost instantaneously, making it difficult to measure the gelation time reliably with a rheometer. When the curing temperature is set at 70°C, the gelation time ranges from 30 min to 52 min. It is evident that the chemical composition has a higher impact on the gelation time at lower temperatures. The viscosity of the AESO/ME mixture with different compositions was tested at different shear rates, and the data are shown in Figure 2-8. For all compositions, the viscosity remains almost constant with increasing shear rate, indicating that both AESO and ME are Newtonian fluids. AESO is a very viscous fluid with a viscosity value around 11 Pa.s. The viscosity of AESO is much greater than regular soybean oil. This is because the AESO contains acrylate and hydroxyl functionality, and these functional groups introduce hydrogen bonding between the triglyceride molecules and increase the viscosity of AESO. As the ME content increased, the viscosity of the resin decreased significantly. ME acts as a reactive diluent in this resin system, making this resin easily processable. On the other hand, a common epoxy system, for example, EPON 828, has a viscosity ranging from 11 Pa.s to 15 Pa.s.

The viscosity of the AESO/ME resin containing 0 wt% to 40 wt% AESO are significantly lower than those of an epoxy system.

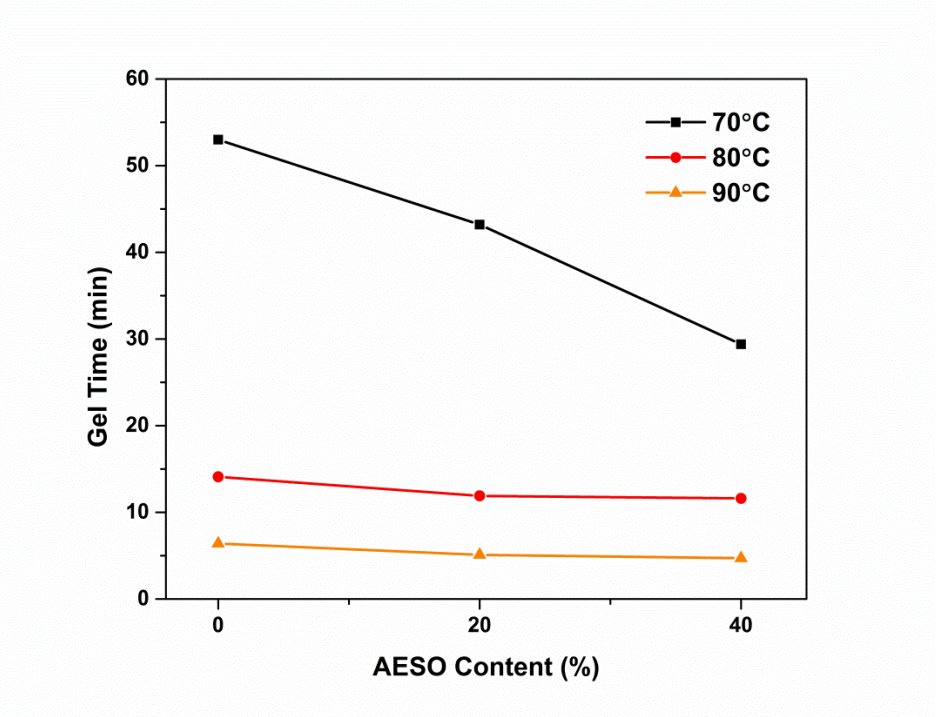

Figure 2-7: Gelation time for AESO/ME copolymers with different compositions cured at 70°C, 80°C, and 90°C.

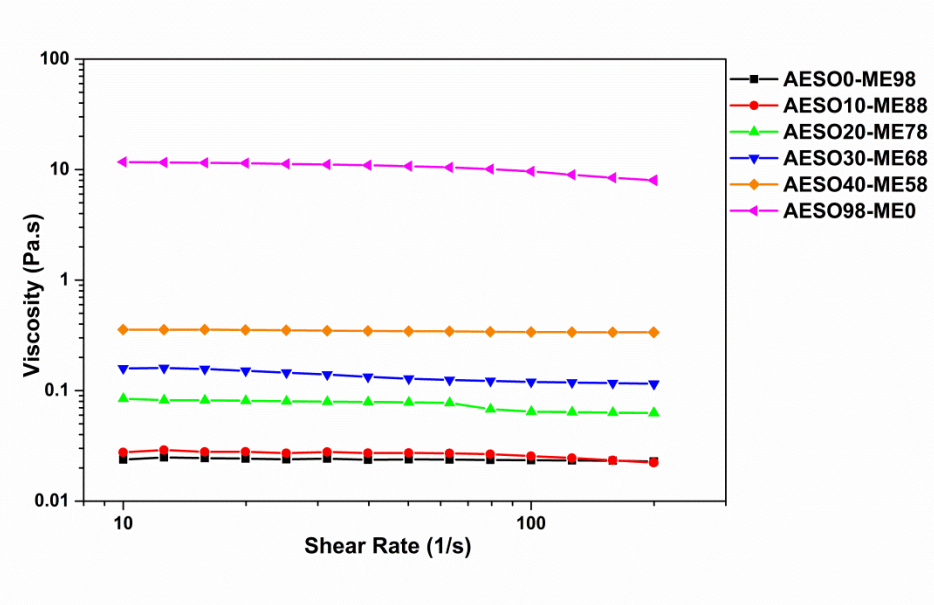

Figure 2-8: Viscosity of AESO/ME copolymers as a function of shear rate.

2.4.5 Thermal properties

Figure 2-9 shows the temperature dependence of storage modulus for AESO/ME copolymer with different compositions. At extremely low temperatures (-100°C to -50°C), all copolymers containing 10 wt% to 40 wt% AESO have similar storage moduli; however, the storage modulus of the pure ME polymer is about 800 MPa higher than those copolymers containing AESO. At a temperature range from 50°C to 150°C, the storage moduli of the copolymers exhibit sharp drops, indicating that glass relaxation, also called α-relaxations, occur at this temperature range. The glass relaxation processes are caused by micro-Brownian motion of the amorphous chains in the thermosetting network; in other words, the segmental mobility of the polymers significantly increases after the glass relaxation process, so that the polymer chains become less rigid. The storage moduli at room temperature for all prepared copolymers are listed in

Table 2-2. Obviously, the storage modulus decreases with increasing AESO content because the incorporation of AESO increases the percentage of long and flexible triglyceride chains in the copolymers system. The ME acts as hard segments in the copolymers because of its aromatic structures, while the ASEO acts as soft segments. By varying the ratio between ME and AESO, the modulus of this copolymer system can be easily tailored to produce either rigid thermoset plastics or softer plastics for different applications. Pure AESO polymer was also tested using the same procedure. Pure AESO polymer possesses much low storage modulus compared to the AESO/ME copolymers.

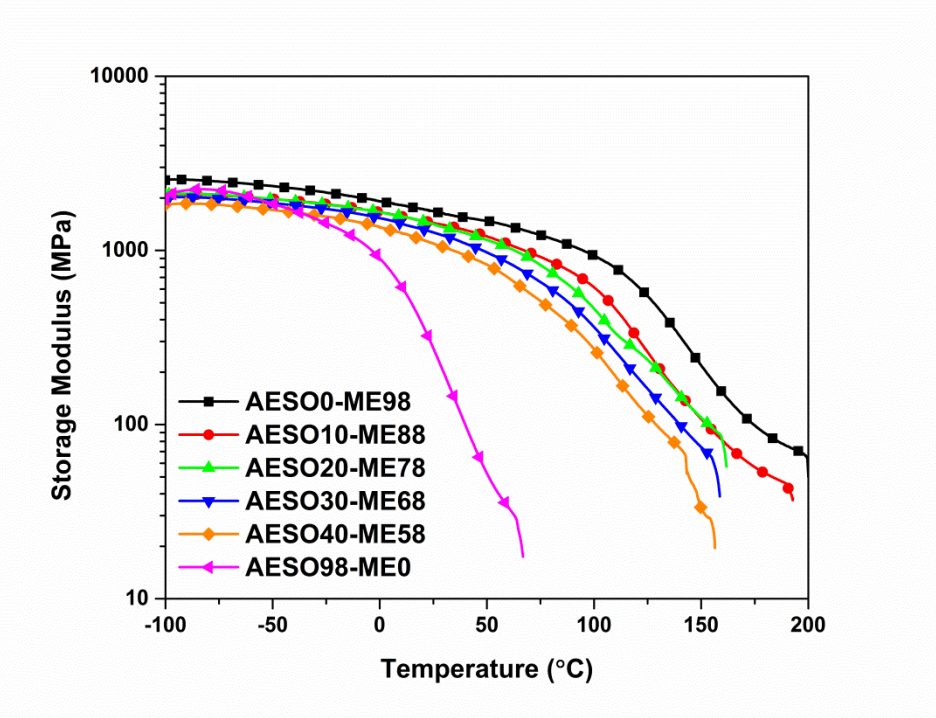

Figure 2-9: Storage moduli for AESO/ME copolymer with different chemical compositions.

Table 2-2: Glass transition temperature and storage modulus at room temperature. The glass transition temperatures is obtained from the maxima the tan δ curves obtained by DMA analysis.

Polymer Composition	Tg [a)] (°C)	E´ at 25°C (MPa)
AESO0-ME98	148.5	1681
AESO10-ME88	136.4	1440
AESO20-ME78	130.2	1411
AESO30-ME68	122.7	1266
AESO40-ME58	121.7	1096
AESO98-ME0	38.2	274

Figure 2-10 depicts the tan δ curve of AESO/ME of different compositions. The tan δ peak is related to the alpha-relaxation of the polymer, and the peak of the tan delta curve is often regarded as the glass transition temperature (T_g). The peaks of the tan δ curves shifted to lower temperatures with increasing amounts of AESO in the resin, indicating that there is more free volume in the copolymer with higher AESO content. This is expected because the triglyceride chains in vegetable oil are bulk and flexible. On the other hand, the ME polymer is relatively rigid due to its aromatic structure. When the soft triglyceride chain is added into ME, the storage moduli and glass transition temperatures of the obtained copolymer are expected to be decreased. Pure ME polymer has a T_g closed to 150°C, which is comparable to most petroleum-based plastics. There is another peak on the tan δ cure of pure ME polymer at 10°C. This peak might be associated with beta relaxation of the thermoset, which corresponds to local relaxation processes of the methacrylate side group. When the AESO content increased from 0 wt% to 10 wt%, the T_g shifted about 12°C to a lower temperature. The drop of T_g is not as pronounced with

high amounts of AESO: the T_g only dropped 1°C when the AESO content increased from 30 wt% to 40 wt%.

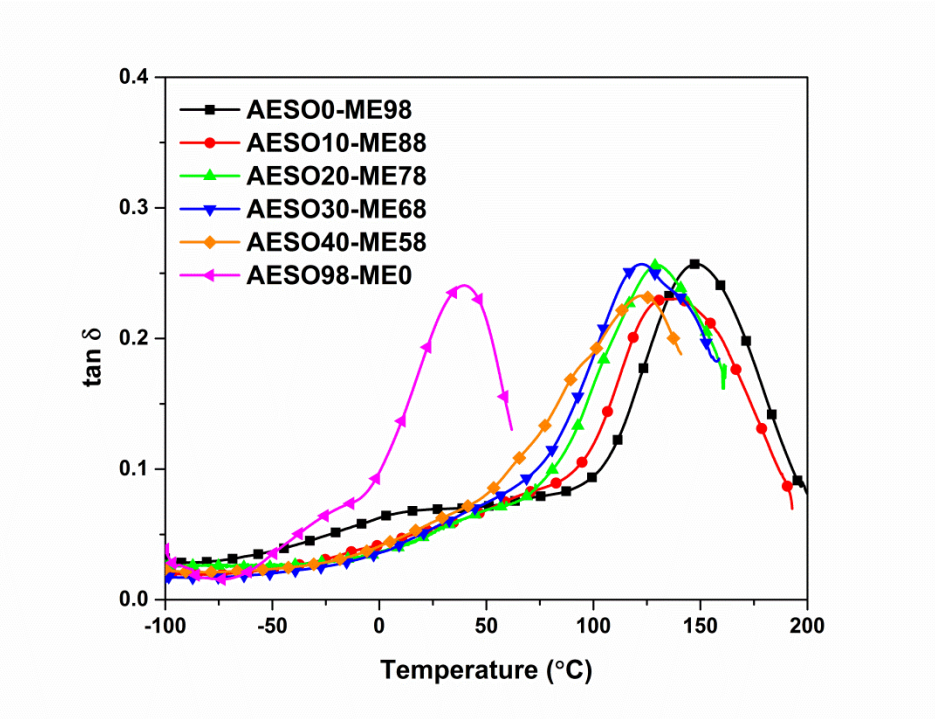

Figure 2-10: Tan δ curves for AESO/ME copolymers with different chemical compositions.

Figure 2-11 and Table 2-3 show the TGA data obtained from the AESO/ME copolymer systems. It is found that all of the copolymers are thermally stable up to 250°C. All of the copolymers exhibit three different stages of thermal degradation above this temperature. The first stage of thermal degradation (250°C to 330°C) is attributed to evaporation and decomposition of some unreacted AESO, unreacted ME, or some low molecular weight portion in the crosslinked structure. The second stage from 330°C to 500°C is the fastest degradation stage, and this degradation stage corresponds to the degradation and char formation of the crosslinked polymer structure. The third stage (above 500°C)

corresponds to the gradual degradation of the char. The thermal stability is essentially the same before the second thermal degradation stage. The T_{10} values (the temperature corresponds to 10% weight loss) of this copolymer system ranges from 370°C to 410°C, and the T_{10} values decrease with an increase in the amount of AESO. The aromatic structure of ME makes ME more thermally stable than the AESO, thereby giving a lower T_{10} value when the ME content decreases. T_{50} (the temperature corresponds to 50% weight loss) and T_{max} (the maximum degradation temperature) also show the same trends as the T_{10} values, indicating that incorporating ASEO into ME decreases the thermal stability at temperatures above 300°C.

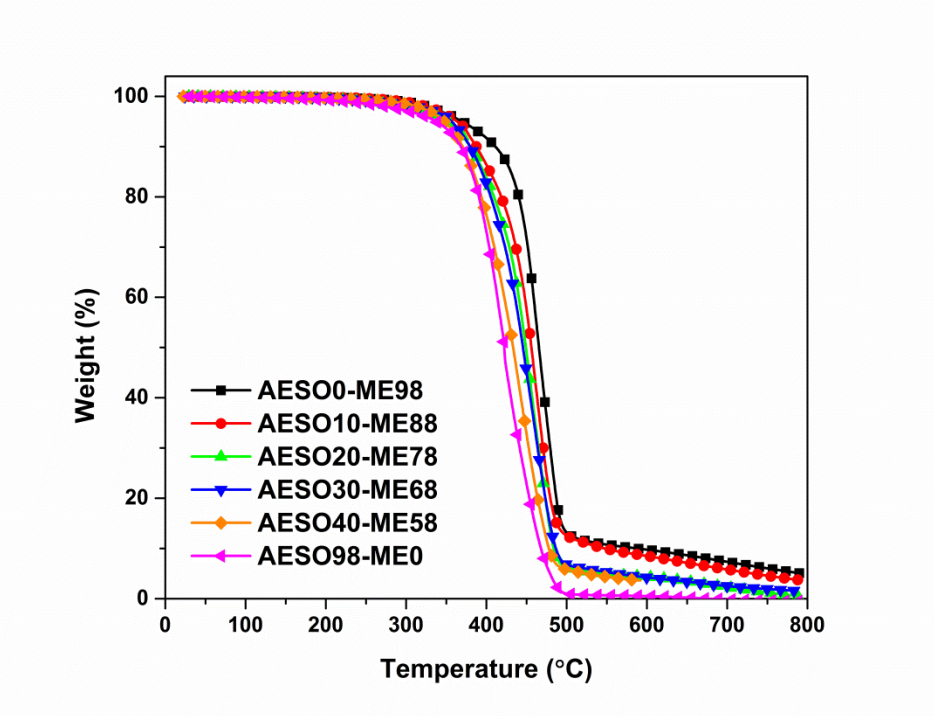

Figure 2-11: TGA measurements for AESO/ME copolymers with different compositions at 20°C/min heating rate under nitrogen atmosphere.

Table 2-3: Important thermal degradation temperature for AESO/ME copolymers.

Polymer Composition	T_{10}	T_{50}	T_{max}
AESO0-ME98	411	465	462
AESO10-ME88	387	456	458
AESO20-ME78	380	449	455
AESO30-ME68	380	446	446
AESO40-ME58	370	433	439
AESO98-ME0	368	422	421

2.4.6 Compression testing

The compressive modulus, ultimate compressive strength, compressive yield strength, and the maximum compressive strength for different copolymers are shown in Figure 2-12 to Figure 2-14 . The compressive modulus is a measure of the stiffness of the material, and it is obtained from calculating the slope of the linear region of the stress vs. strain plot. As expected, the compressive modulus increases with decreasing AESO content because the incorporation of flexible triglyceride molecules will decrease the overall stiffness of the obtained copolymers. The ME polymer possesses a compressive modulus of 2.3 GPA, while the AESO40 copolymer has a compressive modulus of 1.4 GPa. The ultimate compressive strength also follows the same trend as the compressive modulus with variation of AESO content. This is expected because the strength of the copolymers decreases with a decrease in aromatic content. The ultimate compressive strength of the copolymers ranges from 93 MPa for the ME polymer to 70 MPa for the AESO40-ME58 copolymer. The ultimate compressive strength of this bio-based copolymer system exceeds the strength of most petroleum-based thermoplastics, and it is comparable to commercially available thermosets such as epoxies and polyesters. The

yield strength also follows the same trend as the ultimate strength. On the other hand, the maximum compressive strain increases with increasing AESO content, indicating that the triglyceride chains make the copolymer more flexible.

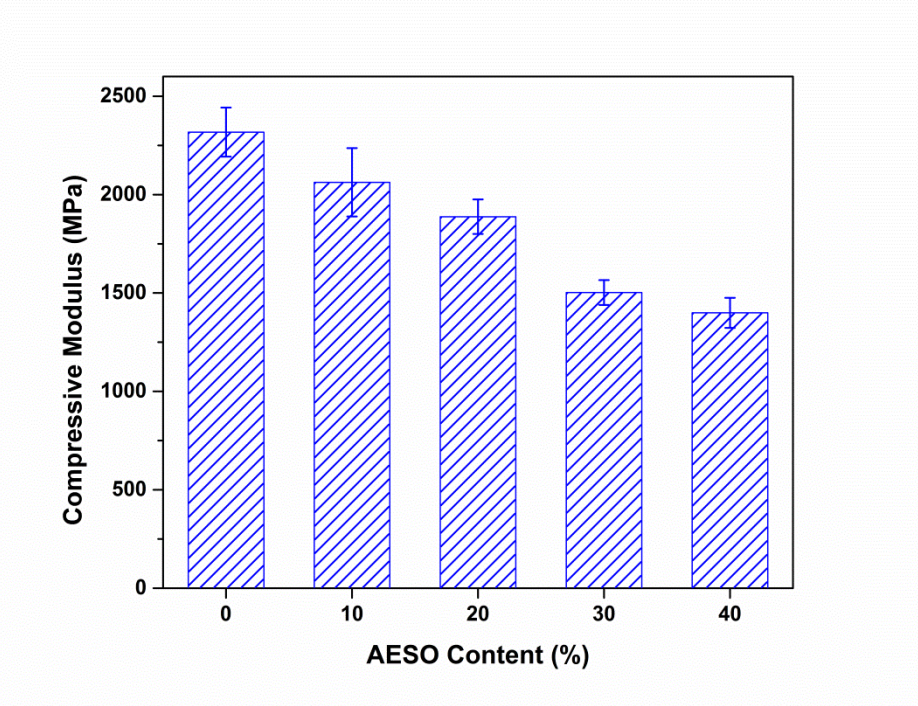

Figure 2-12: Compressive modulus for AESO/ME copolymers with different compositions.

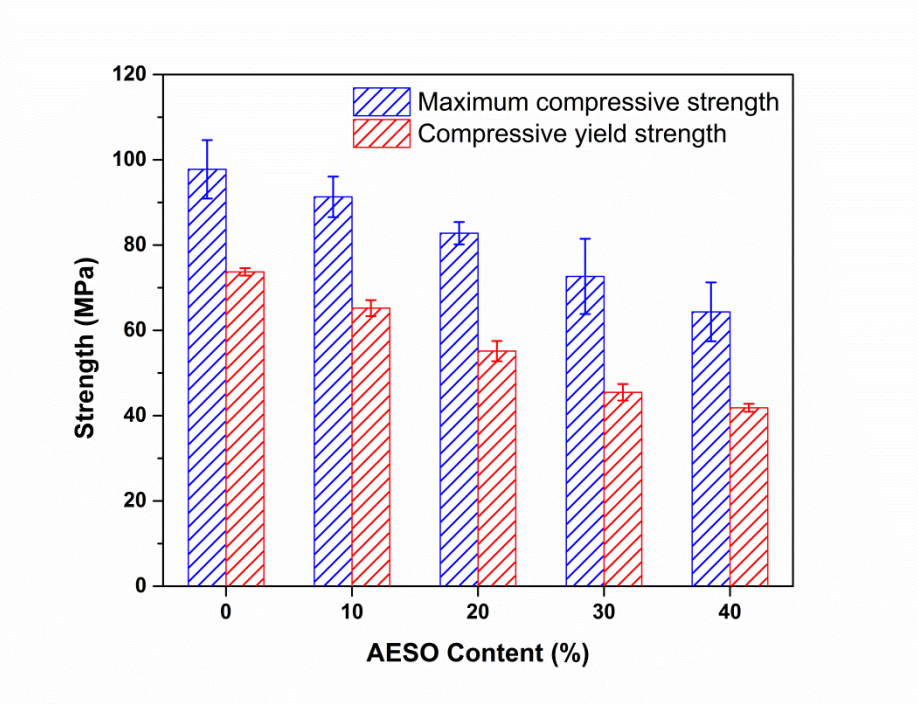

Figure 2-13: Maximum compressive strength and compressive yield strength of AESO/ME copolymers with different compositions.

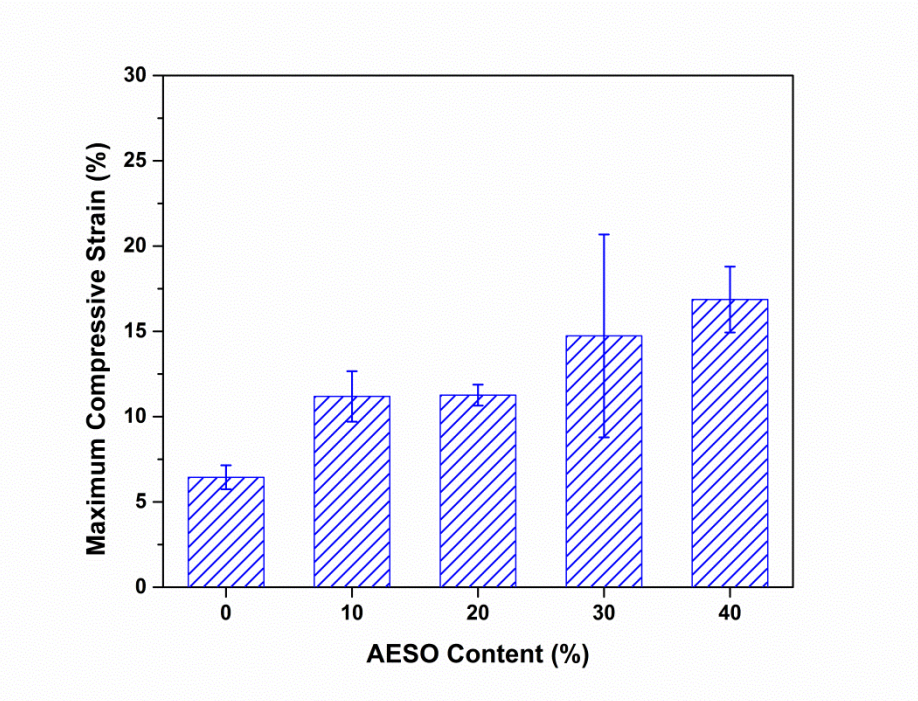

Figure 2-14: Maximum compressive strain for AESO/ME copolymers with different compositions.

2.5 Conclusion

High bio-content thermosetting polymers were prepared using free radical copolymerization of methacrylated eugenol and acrylated epoxidized soybean oil. Both ME and AESO are derived from bio-based chemicals. The bio-based carbon content, which is calculated by dividing the amount of bio-based carbon in the material or product as a weight percentage of the total organic carbon in the material or product [55], was calculated to be ranged from 70.1% (for the AESO0-ME98 sample) to 74.9% (for the AESO40-ME58 sample). This copolymer system was proved to be a suitable candidate for the pultrusion manufacturing process due to its high stiffness and fast gelation time.

All of the obtained copolymers are homogeneous and rigid. Due to the high reactivity of the acrylate functional groups in AESO and the methacrylate functional groups in ME, the insoluble portion of all copolymers were above 95% as evident by the Soxhlet extraction data, indicating that most of the monomers were crosslinked. The high reactivity of the functional groups in AESO and ME and the high decomposition rate of the BPO free radical initiator make the copolymers possess high curing speed. The gelation time is less than 10 minutes when the resin is cured at temperatures above 90°C. The DMA data showed that the storage modulus and the glass transition temperature of the polymers decrease with an increasing percentage of AESO. The compression testing data showed that the modulus and strength decrease with increasing AESO content; however, the ultimate compressive strain was found to increase with an increase in AESO content. TGA data also indicates this copolymer system is thermally stable up to 250°C.

2.6 Acknowledgements

This project was sponsor by the Consortium for Plant Biotechnology Research (CPBR) under the CPBR Agreement EPA83438801-337.

2.7 References

[1] Williams CK, Hillmyer MA. Polymers from renewable resources: A perspective for a special issue of polymer reviews. Polym Rev. 2008;48(1):1-10.

[2] Gandini A. The irruption of polymers from renewable resources on the scene of macromolecular science and technology. Green Chem. 2011;13(5):1061-83.

[3] Xia Y, Larock RC. Vegetable oil-based polymeric materials: synthesis, properties, and applications. Green Chem. 2010;12(11):1893-909.

[4] Li FK, Larock RC. New soybean oil-styrene-divinylbenzene thermosetting copolymers. I. Synthesis and characterization. J Appl Polym Sci. 2001;80(4):658-70.

[5] Andjelkovic DD, Larock RC. Novel rubbers from cationic copolymerization of soybean oils and dicyclopentadiene. 1. Synthesis and characterization. Biomacromolecules. 2006;7(3):927-36.

[6] Valverde M, Andjelkovic D, Kundu PP, Larock RC. Conjugated low-saturation soybean oil thermosets: Free-radical copolymerization with dicyclopentadiene and divinylbenzene. J Appl Polym Sci. 2008;107(1):423-30.

[7] Sharma V, Banait JS, Larock RC, Kundu PP. Morphological and Thermal Characterization of Linseed-Oil Based Polymers from Cationic and Thermal Polymerization. J Polym Environ. 2010;18(3):235-42.

[8] Kundu PP, Larock RC. Novel conjugated linseed oil-styrene-divinylbenzene copolymers prepared by thermal polymerization. 1. Effect of monomer concentration on the structure and properties. Biomacromolecules. 2005;6(2):797-806.

[9] Henna PH, Andjelkovic DD, Kundu PP, Larock RC. Biobased thermosets from the free-radical copolymerization of conjugated linseed oil. J Appl Polym Sci. 2007;104(2):979-85.

[10] Li FK, Hasjim J, Larock RC. Synthesis, structure, and thermophysical and mechanical properties of new polymers prepared by the cationic copolymerization of corn oil, styrene, and divinylbenzene. J Appl Polym Sci. 2003;90(7):1830-8.

[11] Kundu PP, Larock RC. Montmorillonite-Filled Nanocomposites of Tung Oil/Styrene/Divinylbenzene Polymers Prepared by Thermal Polymerization. J Appl Polym Sci. 2011;119(3):1297-306.

[12] Li FK, Larock RC. Thermosetting polymers from cationic copolymerization of tung oil: Synthesis and characterization. J Appl Polym Sci. 2000;78(5):1044-56.

[13] Pfister DP, Baker JR, Henna PH, Lu Y, Larock RC. Preparation and properties of tung oil-based composites using spent germ as a natural filler. J Appl Polym Sci. 2008;108(6):3618-25.

[14] Larock RC, Dong XY, Chung S, Reddy CK, Ehlers LE. Preparation of conjugated soybean oil and other natural oils and fatty acids by homogeneous transition metal catalysis. J Am Oil Chem Soc. 2001;78(5):447-53.

[15] Cai CS, Dai HG, Chen RS, Su CX, Xu XY, Zhang S, et al. Studies on the kinetics of in situ epoxidation of vegetable oils. Eur J Lipid Sci Tech. 2008;110(4):341-6.

[16] Campanella A, Baltanas MA, Capel-Sanchez MC, Campos-Martin JM, Fierro JLG. Soybean oil epoxidation with hydrogen peroxide using an amorphous Ti/SiO2 catalyst. Green Chem. 2004;6(7):330-4.

[17] Miyagawa H, Misra M, Drzal LT, Mohanty AK. Fracture toughness and impact strength of anhydride‐cured biobased epoxy. Polymer Engineering & Science. 2005;45(4):487-95.

[18] Park SJ, Jin FL, Lee JR. Effect of biodegradable epoxidized castor oil on physicochemical and mechanical properties of epoxy resins. Macromol Chem Phys. 2004;205(15):2048-54.

[19] Tan SG, Chow WS. Biobased Epoxidized Vegetable Oils and Its Greener Epoxy Blends: A Review. Polym-Plast Technol. 2010;49(15):1581-90.

[20] Wang CS, Yang LT, Ni BL, Shi G. Polyurethane Networks from Different Soy-Based Polyols by the Ring Opening of Epoxidized Soybean Oil with Methanol, Glycol, and 1,2-Propanediol. J Appl Polym Sci. 2009;114(1):125-31.

[21] Guo A, Cho YJ, Petrovic ZS. Structure and properties of halogenated and nonhalogenated soy-based polyols. J Polym Sci Pol Chem. 2000;38(21):3900-10.

[22] Zhang CQ, Xia Y, Chen RQ, Huh S, Johnston PA, Kessler MR. Soy-castor oil based polyols prepared using a solvent-free and catalyst-free method and polyurethanes therefrom. Green Chem. 2013;15(6):1477-84.

[23] Petrovic ZS. Polyurethanes from vegetable oils. Polym Rev. 2008;48(1):109-55.

[24] Lu J, Khot S, Wool RP. New sheet molding compound resins from soybean oil. I. Synthesis and characterization. Polymer. 2005;46(1):71-80.

[25] Akesson D, Skrifvars M, Walkenstrom P. Preparation of Thermoset Composites from Natural Fibres and Acrylate Modified Soybean Oil Resins. J Appl Polym Sci. 2009;114(4):2502-8.

[26] Khot SN, Lascala JJ, Can E, Morye SS, Williams GI, Palmese GR, et al. Development and application of triglyceride-based polymers and composites. J Appl Polym Sci. 2001;82(3):703-23.

[27] Fu LY, Yang LT, Dai CL, Zhao CS, Ma LJ. Thermal and Mechanical Properties of Acrylated Epoxidized-Soybean Oil-Based Thermosets. J Appl Polym Sci. 2010;117(4):2220-5.

[28] Ramamoorthy SK, Kundu CK, Adekunle K, Bashir T, Skrifvars M. Properties of green composites with regenerated cellulose fiber and soybean-based thermoset for technical applications. J Reinf Plast Comp. 2014;33(2):193-201.

[29] Senoz E, Stanzione JF, Reno KH, Wool RP, Miller MEN. Pyrolyzed Chicken Feather Fibers for Biobased Composite Reinforcement. J Appl Polym Sci. 2013;128(2):983-9.

[30] Sen S, Cayli G. Synthesis of bio-based polymeric nanocomposites from acrylated epoxidized soybean oil and montmorillonite clay in the presence of a bio-based intercalant. Polym Int. 2010;59(8):1122-9.

[31] Zhan MJ, Wool RP. Design and evaluation of bio-based composites for printed circuit board application. Compos Part a-Appl S. 2013;47:22-30.

[32] Zhan MJ, Wool RP. Biobased Composite Resins Design for Electronic Materials. J Appl Polym Sci. 2010;118(6):3274-83.

[33] Basturk E, Inan T, Gungor A. Flame retardant UV-curable acrylated epoxidized soybean oil based organic-inorganic hybrid coating. Prog Org Coat. 2013;76(6):985-92.

[34] Opdyke DLJ, Research Institute for Fragrance Materials. Monographs on fragrance raw materials. Oxford ; New York: Published on behalf of the Research Institute for Fragrance Materials by Pergamon Press; 1979.

[35] Markowitz K, Moynihan M, Liu MS, Kim S. Biologic Properties of Eugenol and Zinc Oxide-Eugenol - a Clinically Oriented Review. Oral Surg Oral Med O. 1992;73(6):729-37.

[36] Duarte GW, Tachinski CG, Naspolini AM, Consenso EC, Salvan RF, Cordova VH, et al. Study of the Processing Conditions Used to Incorporate an Antimicrobial Additive in Thermoplastic Polymer. Advanced Powder Technology Viii, Pts 1 and 2. 2012;727-728:1701-5.

[37] Qin L, Zhang, Wolcott, Zhang. Use of eugenol and rosin as feedstocks for biobased epoxy resins and study of curing and performance properties. 2013.

[38] Rahim EA, Sanda F, Masuda T. Synthesis and properties of a novel polyacetylene containing eugenol moieties. J Macromol Sci Pure. 2004;A41(2):133-41.

[39] Shibata M, Teramoto N, Shimasaki T, Ogihara M. High-performance bio-based bismaleimide resins using succinic acid and eugenol. Polym J. 2011;43(11):916-22.

[40] Telysheva G, Dobele G, Meier D, Dizhbite T, Rossinska G, Jurkjane V. Characterization of the transformations of lignocellulosic structures upon degradation in planted soil. J Anal Appl Pyrol. 2007;79(1-2):52-60.

[41] Kuroda KI, Inoue Y, Sakai K. Analysis of Lignin by Pyrolysis-Gas Chromatography .1. Effect of Inorganic Substances on Guaiacol-Derivative Yield from Softwoods and Their Lignins. J Anal Appl Pyrol. 1990;18(1):59-69.

[42] Varanasi P, Singh P, Auer M, Adams PD, Simmons BA, Singh S. Survey of renewable chemicals produced from lignocellulosic biomass during ionic liquid pretreatment. Biotechnol Biofuels. 2013;6.

[43] Starr TF. Pultrusion for engineers. Boca Raton, FL: CRC Press; 2000.

[44] Safiee S, Akil HM, Mazuki AAM, Ishak ZAM, Abu Bakar A. Properties of Pultruded Jute Fiber Reinforced Unsaturated Polyester Composites. Adv Compos Mater. 2011;20(3):231-44.

[45] Peng X, Fan MZ, Hartley J, Al-Zubaidy M. Properties of natural fiber composites made by pultrusion process. J Compos Mater. 2012;46(2):237-46.

[46] Angelov I, Wiedmer S, Evstatiev M, Friedrich K, Mennig G. Pultrusion of a flax/polypropylene yarn. Compos Part a-Appl S. 2007;38(5):1431-8.

[47] Cui HY. Glass fiber reinforced biorenewable polymer composites and the fabrication with pultrusion process. Thesis Iowa State University. 2013.

[48] Badrinarayanan P, Lu YS, Larock RC, Kessler MR. Cure Characterization of Soybean Oil-Styrene-Divinylbenzene Thermosetting Copolymers. J Appl Polym Sci. 2009;113(2):1042-9.

[49] Chandrashekhara K, Sundararaman S, Flanigan V, Kapila S. Affordable composites using renewable materials. Mat Sci Eng a-Struct. 2005;412(1-2):2-6.

[50] Stanzione JF, Sadler JM, La Scala JJ, Wool RP. Lignin Model Compounds as Bio-Based Reactive Diluents for Liquid M olding Resins. Chemsuschem. 2012;5(7):1291-7.

[51] Burton GW, Ingold KU. Autoxidation of Biological Molecules .1. The Antioxidant Activity of Vitamin-E and Related Chain-Breaking Phenolic Antioxidants Invitro. J Am Chem Soc. 1981;103(21):6472-7.

[52] Fujisawa S, Kadoma Y. Action of eugenol as a retarder against polymerization of methyl methacrylate by benzoyl peroxide. Biomaterials. 1997;18(9):701-3.

[53] Rojo L, Vazquez B, Parra J, Bravo AL, Deb S, Roman JS. From natural products to polymeric derivatives of "eugenol": A new approach for preparation of dental composites and orthopedic bone cements. Biomacromolecules. 2006;7(10):2751-61.

[54] Madbouly SA, Liu KW, Xia Y, Kessler MR. Semi-interpenetrating polymer networks prepared from in situ cationic polymerization of bio-based tung oil with biodegradable polycaprolactone. Rsc Adv. 2014;4(13):6710-8.

[55] AGRICULTURE DO. GUIDELINES FOR DESIGNATING BIOBASED PRODUCTS FOR FEDERAL PROCUREMENT. 7 CFR Part 3201 2012.

CHAPTER 3 : BIORENEWABLE POLYMER COMPOSITES FROM TALL OIL-BASED POLYAMIDE AND LIGNIN-CELLULOSE FIBER

A paper to be submitted to the Journal of Applied Polymer Science

Kunwei Liu[a], Samy A. Madbouly[ab], James A. Schrader[c], Micheal R. Kessler[d], David Grewell[e], and William R. Graves[c]

[a] Department of Materials Science and Engineering, Iowa State University, Ames, IA, USA

[b] Department of Chemistry, Faculty of Science, Cairo University, Orman-Giza, Egypt

[c]Department of Horticulture, Iowa State University, Ames, IA, USA

[d]School of Mechanical and Materials Engineering, Washington State University, Pullman, WA, USA

[e]Department of Agriculture and Biosystems Engineering, Iowa State University, Ames, IA, USA

3.1 Abstract

Tall oil-based polyamide was blended with lignin-cellulose fiber (LCF) to produce environmental-friendly composites. The effects of the concentration of LCF on the thermal, rheological, and mechanical properties of the composites were studied using differential scanning calorimetry (DCS), dynamic mechanical analysis (DMA), thermogravimetric analysis (TGA), rheological testing, and mechanical testing. The morphologies of the composites were investigated using scanning electron microscopy (SEM). The incorporation of LCF does not change the glass relaxation process of the

polyamide significantly. Results from rheological testing showed that the complex viscosity and shear storage modulus were increased by LCF. The modulus and strength both increased with increasing LCF content; however, LCF also dramatically reduced the tensile elongation of the composites. In addition, the thermal stability of the composites was found to be strongly influenced by the concentration of LCF: the onset of the degradation process shifted to lower temperatures with increasing LCF content. Overall, the LCF is a useful filler that is compatible with tall oil-based polyamide. The cost of the composites can be reduced significantly by LCF, while the polyamide matrix can be reinforced by LCF.

3.2 Introduction

Polymers and composites derived from biorenewable resources have received extensive attention as sustainable alternatives to petroleum-based polymers due to the increasing cost of fossil fuels and various environmental concerns. It was estimated that the petroleum resources will be depleted within one hundred years [1]. The traditional petroleum-based polymers are not biorenewable, and most of them are not biodegradable. These widely used petroleum-based polymers have introduced many environmental problems, such as the emission of greenhouse gases and white pollution.

Many thermoplastics and thermosets based on bio-renewable resources have been developed. Polylactide (PLA) is a widely used thermoplastic produced from the fermentation of corn and sugar feedstocks. Because PLA is biorenewable and biodegradable, it has been used in packaging and biomedical applications [2, 3]. On the other hand, polyhydroxyalkanoates (PHA), is a class of polyesters produced from bacteria. Bacteria produce PHA for carbon and energy storage [4]. PHA is biorenewable

and biodegradable, and it also possesses high biocompatibility. PHA has been used as drug carriers and scaffold materials in tissue engineering [5-7]. PHA possesses mechanical properties similar to those of polypropylene; however, the high cost and the brittleness of PHA have limited its applications as a general plastic.

Plant oils, such as soybean oil, castor oil, and tung oil, are very popular starting materials for synthesizing biorenewable thermoplastics and thermosets, since they carry many chemical reactive sites such as double bonds, hydroxyl groups, epoxide groups and ester linkages. Polyamide is a class of polymers that has been widely used in textiles, automotive, electrical, and adhesive application [8]. Some of the most seen polyamides are Nylon 6 and Nylon 6,6, which are produced from petroleum-based chemicals. Polyamides based on vegetable oils have also been synthesized. Polyamide-11, a castor oil-based polyamide produced by Arkema, can be synthesized via polycondensation of 11-aminoundecanoic acid (a fatty acid derived from castor oil). To synthesis 11-aminoundecanoic acid, castor oil is saponified under basic condition and neutralized to produce ricinoleic acid. The ricinoleic acid is then esterified using methanol and ethanol to produce ricinoleic ester. The ester of ricinoleic acid is then heated to 500°C to yield undecylenic acid. The undecylenic acid is then brominated using HBr with the presence of peroxide catalyst, followed by amination reaction using ammonia to yield 11-aminoundecanoic acid – the building block of Polyamide 11 [9]. Another way to synthesis biorenewable polyamide involves the use of vegetable oil-based dimer. Plant oils are first saponified into fatty acids and then converted to dimer acid [10]. The dimer acid contains two carboxylic acid functional groups. Polyamides can be produced after adding diamine to react with the carboxylic acid group from the dimer acid. Hablot et al.

synthesized polyamide based on rapeseed oil dimer acid and 1,2-diaminoehtane, 1,6-diaminohexane or 1,8-diaminooctaine [11]. The obtained polyamides are semi-crystalline polymers with a degree of crystallinity around 10%. The melting points of the resulting polyamide ranges from 79°C to 105°C, and the glass transition temperature was in the range of -17°C to -5°C [11]. This polyamide is soft and flexible with more than 300% maximum tensile strain. Fan et al. prepared a series of polyamide based on soy-based dimer acids with a glass transition temperature as high as 63°C and a modulus value above 2000 MPa [12]. Moreover, polyamides from tung oil and soybean oil have also been synthesized for the paint industry due to their thixotropic rheological properties [13].

Biorenewable polymers are generally inferior to petroleum-based polymer in terms of cost and mechanical properties. For example, PLA and PHA are much more expensive than common petroleum-based polymers such as polyethylene and polystyrene, and they are notorious for their inherent brittleness. A common strategy to compensate the drawbacks of biorenewable polymer is by blending them with fillers or fibers to decrease the overall cost and/or to modify the mechanical properties. There are numerous studies about adding fillers or fibers to biorenewable thermoplastics. Plant fibers such as kenaf fibers, jute fibers, and bamboo fibers, and synthetic fibers such as glass fibers and carbon fibers have been added to PLA [14-18]. Generally, after adding rigid fibers into the PLA matrix, the strength and modulus will both increase if strong interfacial adhesion can be achieved. The effects of organic fillers such as flours, starches, rice straw, lignin, and cellulose on the properties of biorenewable thermoplastics have been extensively studied [19-24]. Moreover, adding agriculture based fillers can

also increase the biodegradation rate of the biodegradable polymers. For example, adding distiller dried grains (DDGS) – a cereal co-product of the corn-ethanol industry into PHA can not only decrease the overall cost of the composites, but also increase the biodegradation rate significantly [25, 26].

There are three major components in the biomass or the cell wall of the plant: lignin, cellulose, and hemicellulose [27, 28]. Lignin is the second most abundant natural resource next to cellulose, and it is a byproduct of the paper and pulp industries and the bio-ethanol industries [29, 30]. Lignin is an amorphous low molecular weight polymer produced from dehydrogenative polymerization of three types of phenols: p-coumaryl, coniferyl and sinapyl alcohols [31, 32]. Lignin makes up about 10 - 30% in wood. In woody plants, lignin offers protection against water, pathogens, pests and enzymatic degradation [27, 31]. Lignin also acts as a binder that holds hemicellulose and cellulose together, providing stiffness to a plant [33]. Lignin has been used as fillers for many thermoplastics. The incorporation of lignin can alter the mechanical properties, thermal stability, and crystallization behavior of the thermoplastics [34-36]. On the other hand, cellulose covers about 45 wt% of dry wood, and it is the most abundant natural material on earth. Cellulose is a polysaccharide consisting of D-glucose linked by β-1,4 linkage [37]. It forms the primary structure component in a plant. Cellulose is a hydrophilic, biodegradable, and semi-crystalline polymer [38]. Hemicellulose is a polysaccharide that makes up 25-30% of wood [37]. It is an amorphous low molecular weight polymer (with molecular weight less than that of cellulose), and it acts as a compatibilizer between cellulose and lignin [39]. Blending plant-based fillers such as cellulose and lignin with

biorenewable plastics can not only produce composites with lower cost, but also increase the biorenewable content and strength of the composites.

The objective of this work is to study the thermal, mechanical, and rheological properties, as well as the morphology of a tall-oil based polyamide reinforced with LCF. The fracture surface morphology was studied using scanning electron microscope (SEM). Dynamic mechanical analysis (DMA) and differential scanning calorimetry (DSC) were performed to study the thermomechanical properties of the PA/LCF composite. Thermogravimetric analysis (TGA) was used to investigate the effect of LCF on the thermal stability of the polyamide. In addition, the rheological behavior of the composites was studied using a rheometer. Standard dog-bone shaped specimens for tensile testing were prepared to investigate the change in yield strength, modulus, and elongation after incorporating LCF into the tall oil-based polyamide.

3.3 Experimental Procedure

3.3.1 Materials

The polyamide (PA) used in this study was UNI-REZ 2651 supplied by Arizona Chemicals (USA). This polyamide is produced based on tall oil-fatty acid dimer. This PA possesses high flexibility with a maximum elongation above 500%. This PA has a softening point around 95 - 105 °C and an amine value of 5. The lignin-cellulose fiber (LCF) was obtained from New Polymer System (New Canaan, CT) in 100-mesh powder form. This filler contains both cellulose and lignin that are extracted from pine trees, and the hemicellulose in the tree is removed by a thermochemical process.

3.3.2 Composite Preparation

Before compounding, PA and LCF were dried at 60°C for 24 h to remove all the moisture. All the composites were prepared by compounding PA with different compositions of LCF using a twin-screw micro-compounder (DACA Instrument, Santa Barbara, CA). The materials were compounded using a rotational speed of 100 rpm for 10 min. The temperature of the barrel was set to 140 °C. The neat PA polymer was also processed using the same conditions so that the samples have the same thermal history. Composites with the following LCF content were prepared: 10 wt%, 20 wt%, 30 wt%. The nomenclature of the composites is presented as follows: PA-20% represents the composites containing 20 wt% of LCF and 80 wt% of PA. The extruded blends were then compression molded using a Carver Model 4394 hydraulic press (Wabash, IN, USA) to form DMA and tensile testing specimens. The temperature and force for compression molding were set to 140°C and 2 tons, respectively. The specimens were cooled to room temperature under pressure before being taken out of the mold.

3.3.3 Morphological characterization

The extruded blends were cryogenically fractured and viewed under an FEI Quanta FEG 250 scanning electron microscopy to examine to morphology the composites. Before the samples were put into the SEM, all samples were sputter coated with a 5nm-thick layer of iridium. The SEM images were taken at a working voltage of 10 kV under high vacuum.

3.3.4 Optical Microscopy

In order to observe the shape of the LCF, the LCF was dispersed in water and put between two parallel glass plates. The sample was then observed using an Olympus BX-51 optical microscope.

3.3.5 DMA measurements

DMA was performed using a Q800 dynamic mechanical analyzer from TA Instrument. Rectangular specimens with a dimension of 30mm × 12.5mm × 1.9 mm from compression molding were used for the DMA measurement. DMA was run in three-point bending mode over the temperature range of -100 to 90°C with a heating rate of 3°C/min, a frequency of 1 Hz, and a displacement amplitude of 20 μm. The storage modulus (E′) and the tan δ were recorded as a function of temperature.

3.3.6 DSC measurements

Differential scanning calorimetry (DSC) was carried out using a TA Instruments Q20 differential scanning calorimeter. All DSC measurements were carried out in a nitrogen atmosphere. The heating and cooling rates for the DSC experiment were set to 30°C/min. A sample weight around 15 to 20 mg was used. Calibration on the DSC machine was performed using an indium sample prior to the experiment. To erase the thermal history, the extruded samples were heated from room temperature to 150 °C. The molten samples were then cooled down to -100°C and heated up again to 150 °C. The second heating run (with no previous thermal history due to processing) was used to study the thermal properties of the PA-LCF composites.

3.3.6 TGA measurements

TGA was carried out using a Q50 thermogravimetric from TA Instrument (New Castle, DE, USA). Samples weighing about 5 mg with different concentrations were heated from 25 °C to 800 °C under a nitrogen atmosphere at a heating rate of 20 °C/ min.

3.3.7 Rheological measurements

The rheological properties of the PA and its composite with LCF were studied using a TA AR2000ex rheometer. Frequency sweeps with 5% strain from 0.1 rad/s and 100 rad/s were performed. The diameter of the plates was 25mm, and the gap between the plates was set to between 0.5mm to 0.6mm. The storage modulus and complex viscosity as a function of angular frequency for composites with different LCF content were studied.

3.3.8 Mechanical testing

The tensile properties of the samples (5 samples for each blend composition) were determined according to ASTM D638 using an Instron 5569 universal testing machine. A load cell with 5 kN capacity was utilized. The tensile testing was conducted at room temperature with a crosshead speed of 50mm/min. The mechanical properties of each composition were determined by averaging the data for at least five samples. The Young’s modulus, yield strength, and strain at break were analyzed as a function of LCF content.

3. 4 Results and Discussion

3.4.1 Optical microscopy and SEM

The LCF is a black substance in its as received form. Optical micrograph of the LCF is shown in Figure 3-1. Most of the LCF was in fiber form, globular form was also observed. The length of the fiber ranges from 60µm to 100µm.

The morphology of the PA/LCF biocomposites was investigated using an SEM. Figure 3-2 shows the cryogenic fracture surface of all prepared compositions. The pure PA polymer shown in Figure 3-2(a) is almost featureless except for some loose polymers resting on top of the surface due to fracture. In Figure 3-2(b), it is evident that the LCF is wetted in the matrix. There are several cavities on the fracture surface, indicating that LCF have been pulled out from the matrix. Figure 3-2(c) and Figure 3-2(d) show that the LCF is homogeneously distributed in the matrix. In addition, there is no gap between the LCF and very few voids are observed, indicating a good interfacial adhesion between the LCF and the matrix.

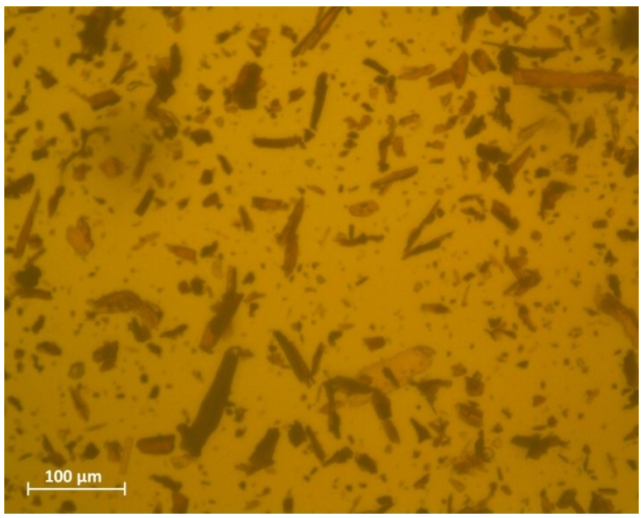

Figure 3-1: Optical micrograph of LCF.

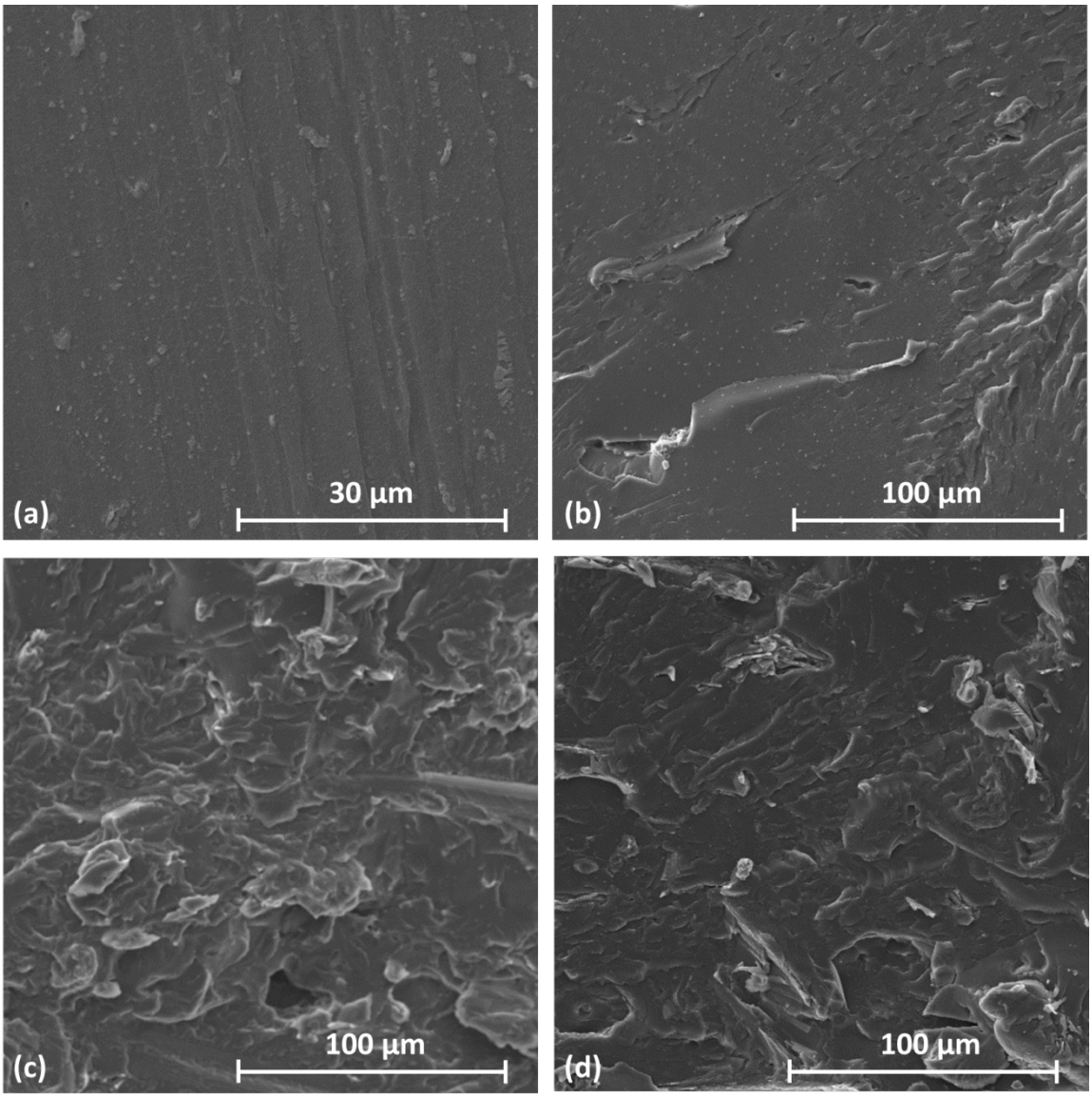

Figure 3-2: SEM images of the fracture surfaces of (a) PA-0%; (b) PA-10%; (c) PA-20%; PA-30%.

3.4.2 Rheology

In order to investigate the effect of LCF on the rheological properties of the composites, composites with different LCF content were tested with a rheometer using a frequency sweep at 140°C. Figure 3-3 depicts the change of shear storage modulus under different angular frequency. The modulus of all sample increased with increasing angular

frequency. It is also apparent that an increase in LCF content increased the shear storage modulus throughout the entire frequency range, which is ascribed to the fact that incorporation of rigid fillers restricts deformation of polymer. For comparison, the storage modulus of PA-30% at 0.1 rad/s is about 5.3 times higher than that of pure PA polymer.

Figure 3-4 shows the evolution of complex viscosity of PA polymer and its composites as a function of angular frequency. As the angular frequency increased, the complex viscosity of all samples were decreased; thus, PA polymer and its composite with LCF exhibit shear thinning behavior (in other words, the material become less resistant to flow as the rate of shear stress increases). The shear thinning behavior was often observed in polymer containing filler particles [25, 40, 41]. The complex viscosity increased when more LCF was added, and this is due to the fact that the rigid LCF filler will decrease the mobility of the polymer chains.

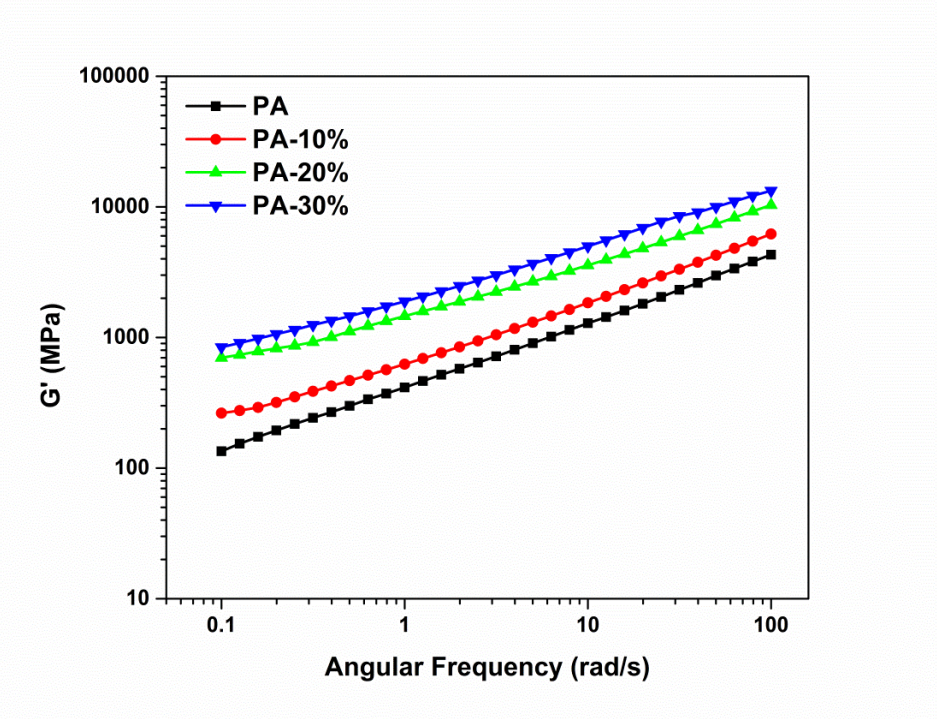

Figure 3-3: Angular frequency dependence of storage modulus at 140°C for PA/LCF composites with different filler contents.

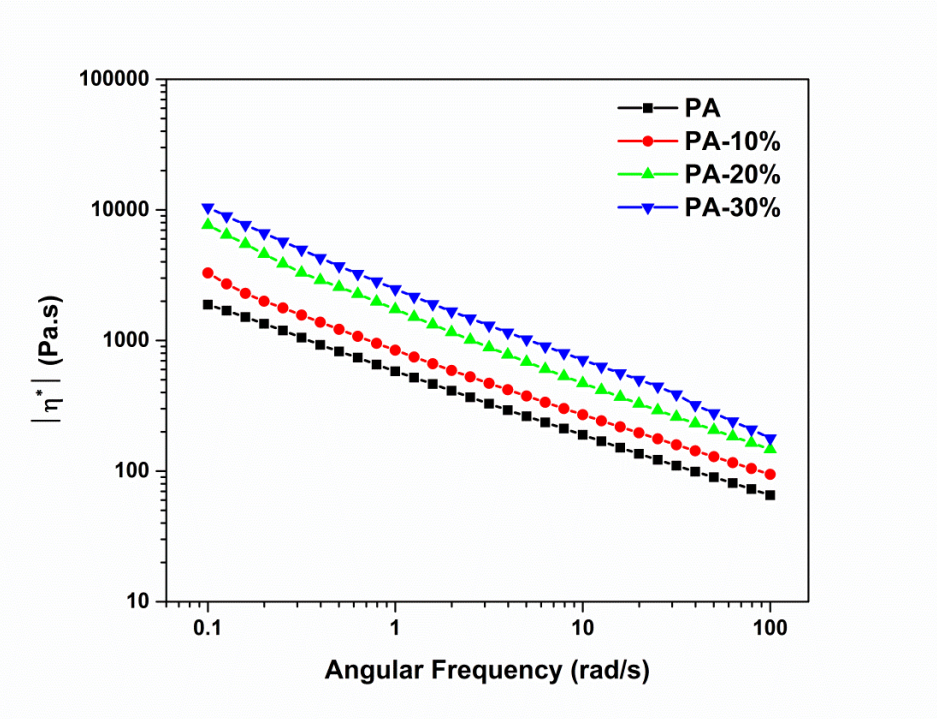

Figure 3-4: Angular frequency dependence of complex viscosity at 140°C for PA/LCF composites with different filler contents.

3.4.3 DMA

The effect LCF content on the storage modulus and the tan δ of the PA/LCF composites were examined by DMA from -100°C to 100°C. Figure 3-5 shows the dynamic storage modulus of the PA/LCF composites as a function of temperature. At temperature below -100°C (glassy region), the storage modulus of the PA polymer was greatly improved by the addition of LCF. The storage modulus of the composites reached the maximum with 20 wt% LCF content. The PA-30 wt% sample has a lower storage modulus at -100°C compared to the composite with 20 wt% LCF, but it has a higher storage modulus than the PA-10% sample, indicating that the reinforcement effect of LCF in the PA matrix reached its maximum at 20 wt% LCF at the glassy region. When the temperature increased to above -50°C, the PA experienced a glass transition relaxation process. A dramatic decrease in storage modulus is evident. At temperatures above 60°C, the storage modulus decreased dramatically again due to the softening of PA at high temperature. On the other hand, the storage modulus at room temperature increased significantly with increasing LCF. For example, the storage modulus of pure PA polymer at room temperature was approximately 90 MPa, while the composite with 30 wt% LCF possesses a modulus about 210 MPa. A 133% increase in storage modulus was observed after adding 30 wt% of LCF. The DMA results correlate well with the tensile testing results that will be shown later in this paper. The increase in modulus is ascribed to the reinforcement effect of the LCF fiber in the soft PA matrix.

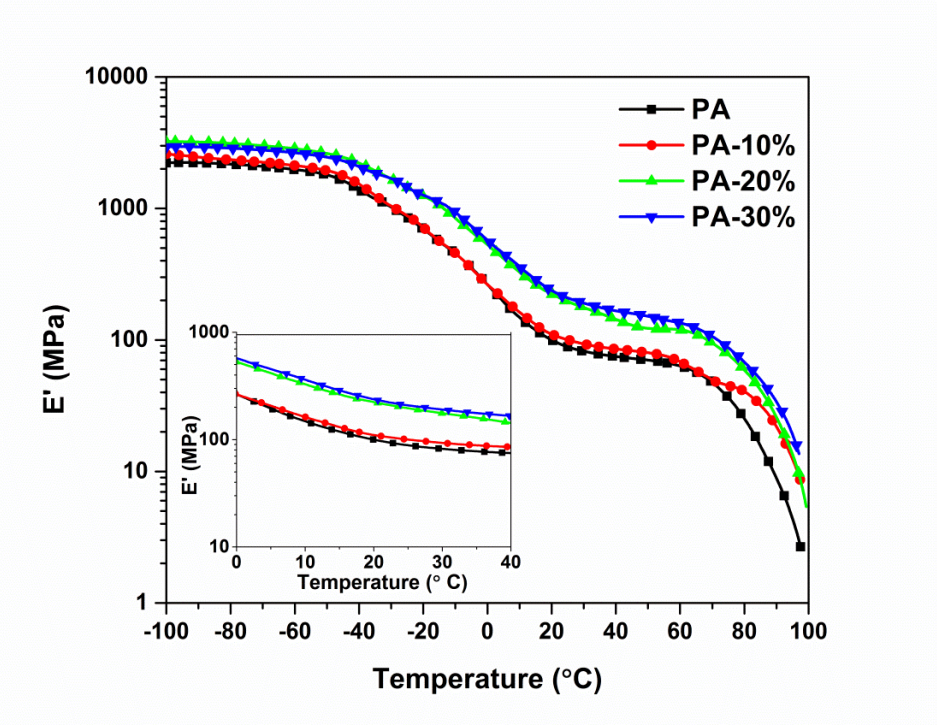

Figure 3-5 : Storage modulus as a function of temperature for the pure PA polymers and its composites with 10wt% to 30 wt% LCF.

The tan δ curves of pure PA and its composite with LCF is shown in Figure 3-6. The broad tan δ peak in the range of -20°C to 50°C is associated with the glass transition process (α-relaxation process) of the PA. The glass transition process indicates the rapid increase of the sliding movement of the amorphous polymeric chains in PA due to high temperatures. The temperature corresponding to the maxima of the tan δ is generally considered the glass transition temperature (T_g). The glass transition temperature of all prepared composites ranged from 5.7 °C to 7.2 °C. It is clear that the concentration of LCF has little effect on the glass transition temperature of the composites. The PA-30% composite showed a 1.5°C increase in the glass transition temperature compared to pure PA polymer. On the other hand, the tan δ curves of all composites exhibited a shoulder at approximately -40°C. The shoulders were located at a constant temperature regardless of

LCF content. The shoulder at this temperature is ascribed to the β-relaxation of the polyamide matrix. β-relaxation is caused by the rotation movement of the side groups and some loosely packed chain segments of PA [42]. The area under the tan δ curve of pure PA is larger than those of PA/LCF composites, indicating that the damping ability of the composites is worse than that of pure PA. This is also expected because adding rigid LCF into the soft PA matrix will decrease the mobility of PA polymeric chain.

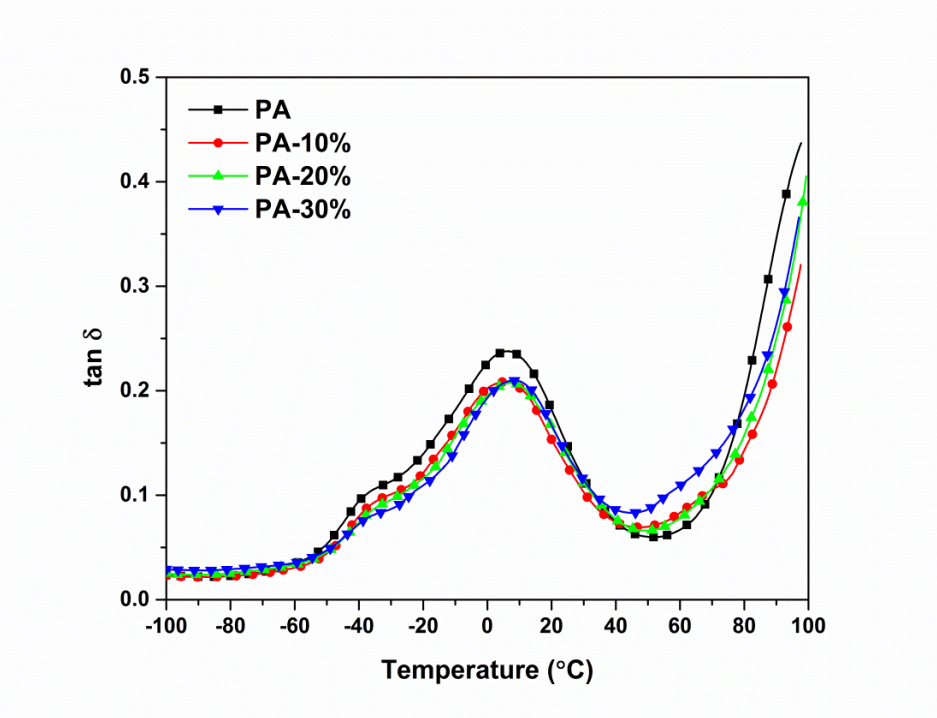

Figure 3-6: Tan δ curves as a function of temperature obtained via DMA.

3.4.4 DSC

DSC was performed to study the effect of LCF on the thermal behavior of composite, particularly the melting point and glass transition temperature. Figure 3-7 shows the DSC traces of pure PA polymer and PA-LCF composites during the second heating run (after all the thermal history had been removed). For this material, there is a very broad glass

transition from -56°C to -10°C. The glass transition temperature is around 33°C, regardless of composition. There is an endothermic peak at about 80 to 90°C, which is associated with the melting of the crystalline region in the PA polymer. The location of melting peaks shifted slightly to higher temperatures as the content of LCF increased, indicating that the LCF may act as a crystallization nucleating agents for PA polymer.

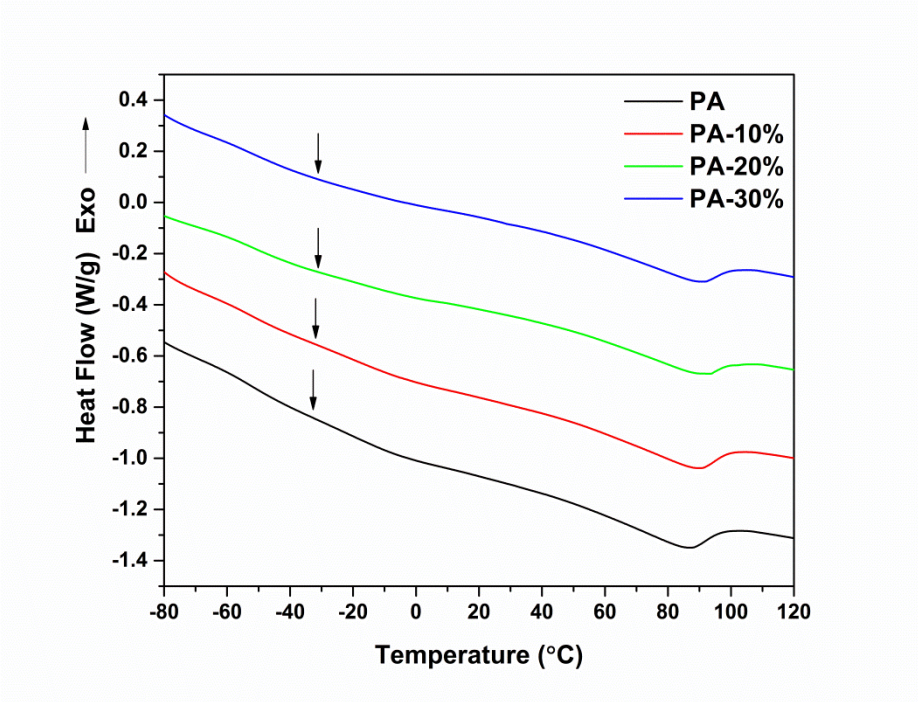

Figure 3-7: DSC traces of PA polymer and composites containing 10 wt% to 30 wt% of LCF.

3.4.5 TGA

The thermal degradation behaviors of the PA/LCF composites were studied using TGA. Figure 3-8 shows the TGA measurement for PA/LCF composites with different LCF content. PA polymer undergoes a major thermal degradation at approximately 355°C, and it lost almost all its original mass at 450°C. On the other hand, the pure LCF started to

degrade at a temperature around 290°C, and the degradation rate of lignin decreased dramatically when the temperature reached 345°C. Table 3-1 presents the temperatures corresponding to the 5% weight loss (T_5), the temperatures corresponding the 10% weight loss (T_{10}), the onset degradation temperature (T_{onset}), and the maximum degradation temperature of all samples (T_{max}). After comparing the thermal degradation behavior of composites with different content of LCF, it is clear that when more LCF was added, the onset degradation temperature, T_5 and T_{10} shifted at a lower temperature. This indicates that increasing LCF content decreases the thermal stability of the composite at the temperature range between 250°C and 400°C. Figure 3-9 shows an enlarged view at the 250°C to 400°C region of Figure 3-8. The onset temperatures of thermal degradation for composites containing 0%, 10%, 20%, and 30% are 355°C, 342°C, 336°C, and 320°C respectively. Due to the aromatic chemical structure of lignin, the thermal stability of the overall composites at the temperature between 400°C to 800°C was greatly increased with increasing LCF content.

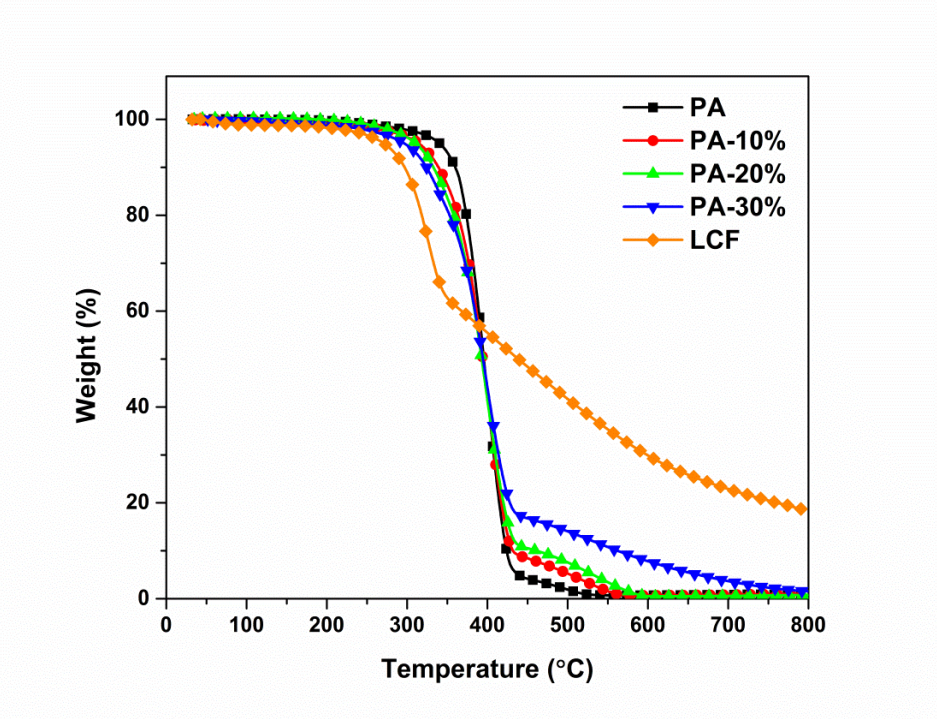

Figure 3-8: Thermal degradation behavior of pure PA polymer, the pure LCF, and their composites.

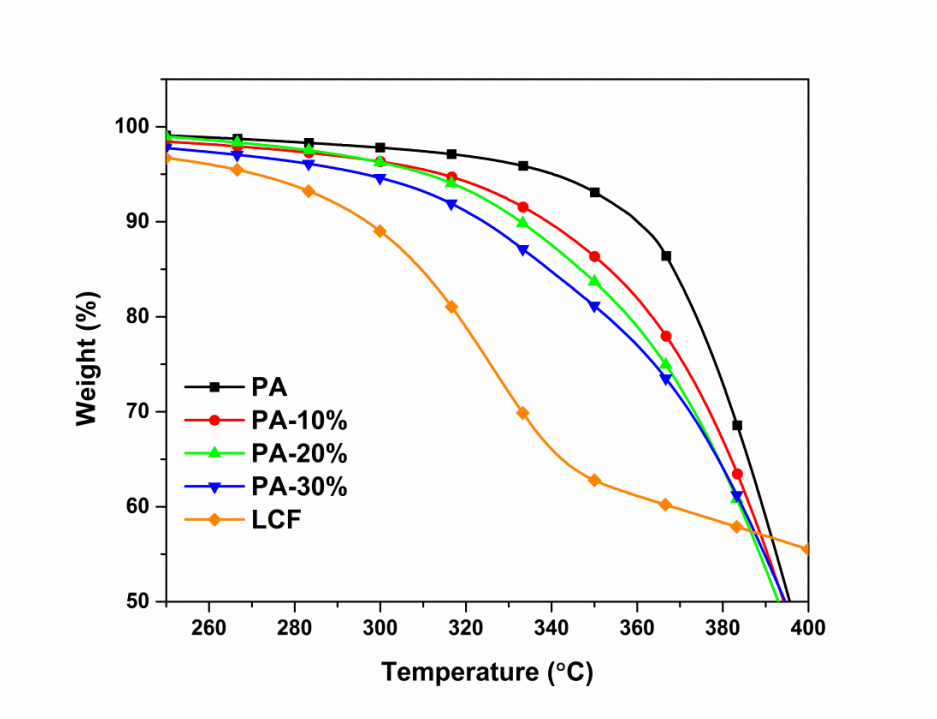

Figure 3-9: Enlarged portion of Figure 3-8 showing details about the onset of thermal degradation.

Table 3-1: Important degradation temperature obtained from TGA.

Samples	T_5(°C)	T_{10}(°C)	T_{onset}(°C)	T_{max} (°C)
PA	340	360	355	400
PA-10%	314	339	342	400
PA-20%	312	333	336	399
PA-30%	296	324	320	399
LCF	271	297	296	326

Figure 3-10 illustrates the derivative rate of weight loss for all the samples. The peaks in this figure are an indication of the temperature at which the maximum thermal degradation rate is achieved. According to Figure 3-10, the largest peaks of the weight derivative curve for PA and its composites are all at 400°C, regardless of the composition.

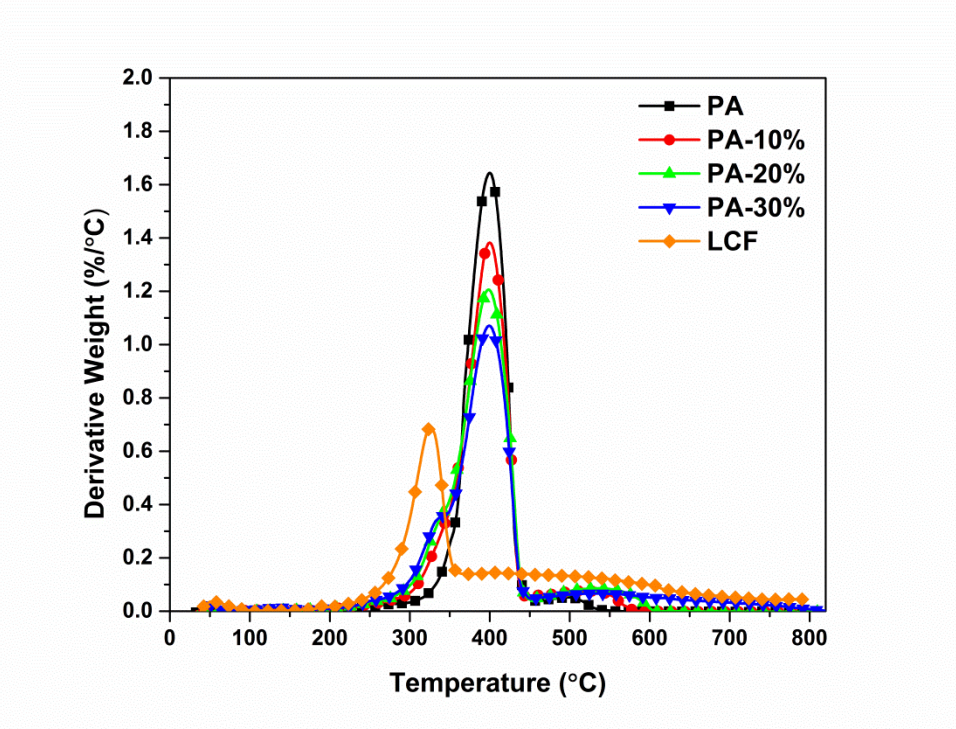

Figure 3-10: Weight derivative of pure PA polymer, LCF, and their composites.

3.4.6 Mechanical testing

Figure 3-11, Figure 3-12, and Figure 3-13 show the mechanical properties of the resulting composites, namely the modulus, yield strength, and strain at break, respectively. The data revealed that the Young's modulus increased with increasing amount of LCF. The PA-30% composite possess a modulus value of 188 MPa, while the Young's modulus of the pure PA polymer was about 90 MPa. The modulus of the composites was doubled by adding 30 wt% LCF. Nitz et al. [43] also found similar results: adding LCF into polyamide-11 led to a systematic increase in Young's modulus of the resulting composites; however, adding 30 wt% LCF into polyamide-11 only yielded about 35% increase in modulus. The yield strength of the composites was also compared as a function of LCF content. From Figure 3-12, it is clear that the yield strength increases with increasing filler content. The strength of the pure PA is about 3.3 MPa in comparison to 6.1 MPa for the PA-30% composite. The increase of both Young's modulus and yield strength is probably attributed to the good dispersion of LCF and the good interfacial interaction between the fillers and the PA matrix [44]. The strain at break for the composites is shown in Figure 3-13. The PA polymer is a highly stretchable polymer that possesses a maximum strain about 600%. As the LCF content increases, the strain at break decreased significantly. The most dramatic drop is observed when the LCF content increased from 0% to 10% – the strain at break of the PA-10% composite dropped 70% compared to the pure PA polymer. For the PA-30% sample, the strain at break of the composite was only 47%. The dramatic drop of maximum strain is common in polymers filled with rigid fillers, because each filler particle will decrease the mobility of the polymer chain when under an applied load. In addition, there is a tendency for the

fillers to agglomerate, which will further decrease the elongation of the resulting composite. In conclusion, the addition of LCF increases the modulus and strength of the composite; however, LCF also embrittles the PA polymer.

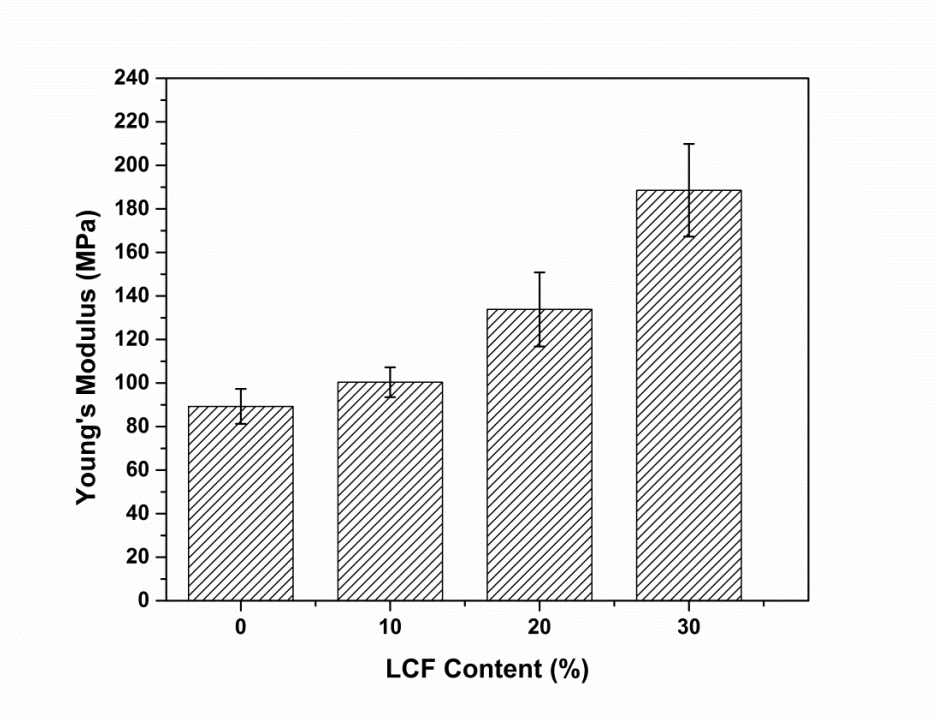

Figure 3-11: Young's modulus as a function of LCF content.

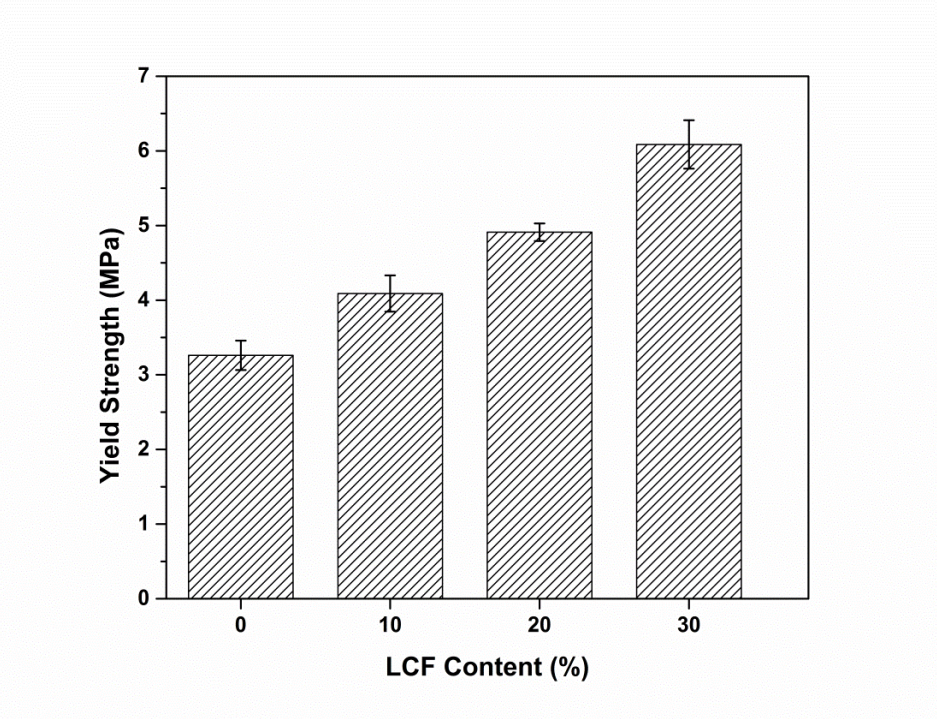

Figure 3-12: Yield Strength as a function of LCF content.

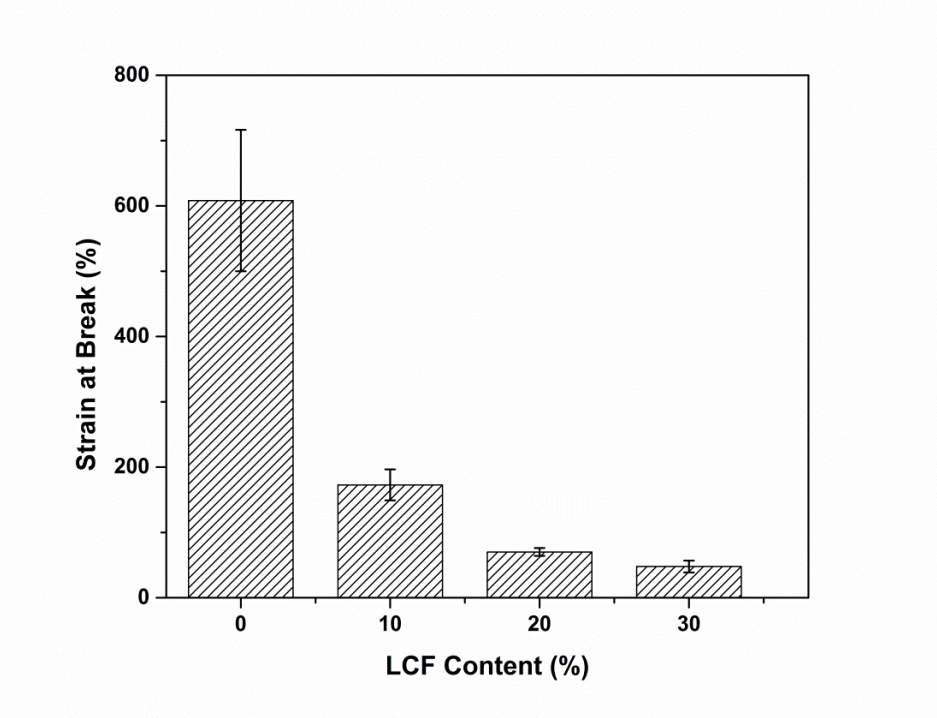

Figure 3-13: Strain at break as a function of LCF content.

3.4 Conclusions

Tall oil-based polyamide was blended with lignin-cellulose fiber (a type of fiber that contains both cellulose and lignin) to produced biocomposites. The effects of LCF on the thermal, mechanical, and rheological properties have been investigated. DMA results indicated that the glass transition temperatures were only slightly affected by the addition of LCF. DMA results also showed that the storage modulus at room temperature increased with increasing amount of LCF. The enhancement in storage modulus indicated that the reinforcement effect of the LCF fiber. TGA test was performed to study the thermal degradation behavior, and the TGA data showed that LCF decrease the thermal stability of the composites at the 250°C - 400°C range. The dynamic viscosity and shear modulus increased significantly with the increasing LCF content. Tensile testing was used to investigate the mechanical properties of the PA/LCF composites. The Young's modulus and yield strength increased with the additional of LCF, but the strain at break was reduced. To conclude, this paper demonstrates that the lignin-cellulose fiber can be blended with tall oil-based polyamides via melt processing to produce biorenewable composites with lower cost, higher mechanical properties, and higher biorenewable content.

3.5 Acknowledgements

This study was funded by the USDA Specialty Crops Research Initiative (USDA-SCRI project # IOW05306).

3.6 References

[1] Williams CK, Hillmyer MA. Polymers from renewable resources: A perspective for a special issue of polymer reviews. Polym Rev. 2008;48(1):1-10.

[2] Mills CA, Navarro M, Engel E, Martinez E, Ginebra MP, Planell J, et al. Transparent micro- and nanopatterned poly(lactic acid) for biomedical applications. J Biomed Mater Res A. 2006;76A(4):781-7.

[3] Auras R, Harte B, Selke S. An overview of polylactides as packaging materials. Macromol Biosci. 2004;4(9):835-64.

[4] Zinn M, Witholt B, Egli T. Occurrence, synthesis and medical application of bacterial polyhydroxyalkanoate. Adv Drug Deliver Rev. 2001;53(1):5-21.

[5] Pouton CW, Akhtar S. Biosynthetic polyhydroxyalkanoates and their potential in drug delivery. Adv Drug Deliver Rev. 1996;18(2):133-62.

[6] Sendil D, Gursel I, Wise DL, Hasirci V. Antibiotic release from biodegradable PHBV microparticles. J Control Release. 1999;59(2):207-17.

[7] Kassab AC, Piskin E, Bilgic S, Denkbas EB, Xu K. Embolization with polyhydroxybutyrate (PHB) microspheres: In-vivo studies. J Bioact Compat Pol. 1999;14(4):291-303.

[8] Martino L, Basilissi L, Farina H, Ortenzi MA, Zini E, Di Silvestro G, et al. Bio-based polyamide 11: Synthesis, rheology and solid-state properties of star structures. Eur Polym J. 2014;59(0):69-77.

[9] Karak N. Vegetable oil-based polymers properties, processing and applications. Cambridge, UK ; Philadelphia: Woodhead Publishing; 2012.

[10] Cavus S, Gurkaynak MA. Influence of monofunctional reactants on the physical properties of dimer acid-based polyamides. Polym Advan Technol. 2006;17(1):30-6.

[11] Kolb N, Winkler M, Syldatk C, Meier MAR. Long-chain polyesters and polyamides from biochemically derived fatty acids. Eur Polym J. 2014;51:159-66.

[12] Fan XD, Deng YL, Waterhouse J, Pfromm P. Synthesis and characterization of polyamide resins from soy-based dimer acids and different amides. J Appl Polym Sci. 1998;68(2):305-14.

[13] Oldring PKT, SITA Technology Limited. Resins for surface coatings. 2nd ed. Chichester ; New York: Wiley; 2000.

[14] Tokoro R, Vu DM, Okubo K, Tanaka T, Fujii T, Fujiura T. How to improve mechanical properties of polylactic acid with bamboo fibers. J Mater Sci. 2008;43(2):775-87.

[15] Huda MS, Drzal LT, Mohanty AK, Misra M. Effect of fiber surface-treatments on the properties of laminated biocomposites from poly(lactic acid) (PLA) and kenaf fibers. Compos Sci Technol. 2008;68(2):424-32.

[16] Ma H, Joo CW. Structure and mechanical properties of jute-polylactic acid biodegradable composites. J Compos Mater. 2011;45(14):1451-60.

[17] Ahmed I, Cronin PS, Abou Neel EA, Parsons AJ, Knowles JC, Rudd CD. Retention of Mechanical Properties and Cytocompatibility of a Phosphate-Based Glass Fiber/Polylactic Acid Composite. J Biomed Mater Res B. 2009;89B(1):18-27.

[18] Wan YZ, Wang YL, Li QY, Dong XH. Influence of surface treatment of carbon fibers on interfacial adhesion strength and mechanical properties of PLA-based composites. J Appl Polym Sci. 2001;80(3):367-76.

[19] Mathew AP, Oksman K, Sain M. Mechanical properties of biodegradable composites from poly lactic acid (PLA) and microcrystalline cellulose (MCC). J Appl Polym Sci. 2005;97(5):2014-25.

[20] Garcia M, Garmendia I, Garcia J. Influence of natural fiber type in eco-composites. J Appl Polym Sci. 2008;107(5):2994-3004.

[21] Kim KW, Lee BH, Kim HJ, Sriroth K, Dorgan JR. Thermal and mechanical properties of cassava and pineapple flours-filled PLA bio-composites. J Therm Anal Calorim. 2012;108(3):1131-9.

[22] Gordobil O, Egüés I, Llano-Ponte R, Labidi J. Physicochemical properties of PLA lignin blends. Polym Degrad Stabil. 2014;108(0):330-8.

[23] Buzarovska A, Bogoeva-Gaceva G, Grozdanov A, Avella M, Gentile G, Errico M. Potential use of rice straw as filler in eco-composite materials. Aust J Crop Sci. 2008;1(2):37-42.

[24] Lee JA, Yoon MJ, Lee ES, Lim DY, Kim KY. Preparation and characterization of cellulose nanofibers (CNFs) from microcrystalline cellulose (MCC) and CNF/polyamide 6 composites. Macromol Res. 2014;22(7):738-45.

[25] Lu H, Madbouly SA, Schrader JA, Kessler MR, Grewelle D, Graves WR. Novel bio-based composites of polyhydroxyalkanoate (PHA)/distillers dried grains with solubles (DDGS). Rsc Adv. 2014;4(75):39802-8.

[26] Madbouly SA, Liu KW, Xia Y, Kessler MR. Semi-interpenetrating polymer networks prepared from in situ cationic polymerization of bio-based tung oil with biodegradable polycaprolactone. Rsc Adv. 2014;4(13):6710-8.

[27] Achyuthan KE, Achyuthan AM, Adams PD, Dirk SM, Harper JC, Simmons BA, et al. Supramolecular Self-Assembled Chaos: Polyphenolic Lignin's Barrier to Cost-Effective Lignocellulosic Biofuels. Molecules. 2010;15(12):8641-88.

[28] Yang HP, Yan R, Chen HP, Zheng CG, Lee DH, Liang DT. In-depth investigation of biomass pyrolysis based on three major components: Hemicellulose, cellulose and lignin. Energ Fuel. 2006;20(1):388-93.

[29] Solomon BD, Barnes JR, Halvorsen KE. Grain and cellulosic ethanol: History, economics, and energy policy. Biomass Bioenerg. 2007;31(6):416-25.

[30] Thielemans W, Wool RP. Butyrated kraft lignin as compatibilizing agent for natural fiber reinforced thermoset composites. Compos Part a-Appl S. 2004;35(3):327-38.

[31] Laurichesse S, Averous L. Chemical modification of lignins: Towards biobased polymers. Prog Polym Sci. 2014;39(7):1266-90.

[32] Mohanty AK, Misra M, Drzal LT. Sustainable bio-composites from renewable resources: Opportunities and challenges in the green materials world. J Polym Environ. 2002;10(1-2):19-26.

[33] Boudet AM, Kajita S, Grima-Pettenati J, Goffner D. Lignins and lignocellulosics: a better control of synthesis for new and improved uses. Trends Plant Sci. 2003;8(12):576-81.

[34] Liu CH, Xiao CB, Liang H. Properties and structure of PVP-lignin "blend films". J Appl Polym Sci. 2005;95(6):1405-11.

[35] Canetti M, Bertini F, De Chirico A, Audisio G. Thermal degradation behaviour of isotactic polypropylene blended with lignin. Polym Degrad Stabil. 2006;91(3):494-8.

[36] Kai WH, He Y, Asakawa N, Inoue Y. Effect of lignin particles as a nucleating agent on crystallization of poly(3-hydroxybutyrate). J Appl Polym Sci. 2004;94(6):2466-74.

[37] Pérez J, Munoz-Dorado J, de la Rubia T, Martinez J. Biodegradation and biological treatments of cellulose, hemicellulose and lignin: an overview. International Microbiology. 2002;5(2):53-63.

[38] Gandini A. The irruption of polymers from renewable resources on the scene of macromolecular science and technology. Green Chem. 2011;13(5):1061-83.

[39] Hansen CM, Bjorkman A. The ultrastructure of wood from a solubility parameter point of view. Holzforschung. 1998;52(4):335-44.

[40] Marcovich NE, Reboredo MM, Kenny J, Aranguren MI. Rheology of particle suspensions in viscoelastic media. Wood flour-polypropylene melt. Rheol Acta. 2004;43(3):293-303.

[41] Madbouly SA, Schrader JA, Srinivasan G, Liu KW, McCabe KG, Grewell D, et al. Biodegradation behavior of bacterial-based polyhydroxyalkanoate (PHA) and DDGS composites. Green Chem. 2014;16(4):1911-20.

[42] Madbouly SA, Otaigbe JU, Ougizawa T. Morphology and properties of novel blends prepared from simultaneous in situ polymerization and compatibilization of macrocychc carbonates and maleated poly(propylene). Macromol Chem Phys. 2006;207(14):1233-43.

[43] Nitz H, Semke H, Mulhaupt R. Influence of lignin type on the mechanical properties of lignin based compounds. Macromol Mater Eng. 2001;286(12):737-43.

[44] Hablot E, Matadi R, Ahzi S, Averous L. Renewable biocomposites of dimer fatty acid-based polyamides with cellulose fibres: Thermal, physical and mechanical properties. Compos Sci Technol. 2010;70(3):504-9.

CHAPTER 4: GENERAL CONCLUSION

4.1 Summary

Chapter 1 presents a literature review of vegetable oil-based vinyl thermosets and the future trends of biorenewable polymers. As the petroleum resources are running out day-by-day, it is urgent to put more and more efforts in developing better biorenewable polymers. Even though most of the biorenewable polymers nowadays are either too expensive and/or possess inferior performance when compared to petroleum-based polymers, I believe that continuous research activities in this field will eventually discovered various biorenewable polymers that can be widely used in many applications, including general plastics to high-end applications such as aerospace and military industries. The literature review in Chapter 1 covers some major discoveries in vegetable oil-based vinyl thermosets. Dr. Larock's group from Iowa State University developed many thermosets based on conjugated vegetable oils and various petroleum-based monomers such as styrene, divinylbenzene, dicyclopentadiene. Dr. Wool's group from University of Delaware prepared a wide range of thermosets based on glycerolysis of vegetable oils and chemical modification using anhydrides.

A novel thermosetting polymer based on modified soybean oil and a modified eugenol was discussed in Chapter 2. Both soybean oil and eugenol used in this study are bio-based; however, to render soybean oil and eugenol polymerizable, modifications must be performed to attach acrylate groups on soybean oil and methacrylate groups9 on eugenol. The original intent of this project was to develop a vegetable oil-based polymer

for pultrusion process. After extensive material characterizations, it was found that this resin system is suitable for pultrusion process, because it has high curing speed and high stiffness. At a curing temperature above 90°C, a rigid thermoset can be produced within several minutes, which is a desired property for large scale manufacturing. Most of the vegetable oil-based thermosets presented in literatures either requires solvent of a long curing time. Producing a thermoset with a longer curing time in a manufacturing setting requires more energy, more space, and eventually leading to higher production cost and less profit. The short curing time for the AESO/ME resin system makes it easily implementable in large-scale manufacturing. In addition, this resin system contains very high biorenewable content – about 70% of carbon atoms in the thermosets are originated from biorenewable resources. On the other hand, AESO and ME are less toxic when comparing to common petroleum-based monomers such as styrene and methyl methacrylate.

Thermosets based on only methacrylated eugenol are too expensive and brittle, and copolymerizing ME with AESO can reduce the cost and increase the toughness of the copolymers. However, thermosets based on only ASEO are too viscous to process. A combination of AESO and ME can yield thermosets with a wide range of mechanical properties and reasonable viscosities. In this resin system, ME imparts stiffness and strength, while AESO imparts flexibility.

Although this resin system possesses many advantages, it is far from ideal. A comparison of mechanical properties between this resin and many other petroleum-based thermoplastics and thermosets indicated that while this resin possesses higher strength and modulus when comparing to thermoplastics, its performance is inferior to traditional

thermosets such as polyesters and epoxies. Price is also a big drawback for this resin. Eugenol is considered an essential oil nowadays, and its price is very high. Fortunately, there are studies that focus on pyrolysis or depolymerization of lignin to produce eugenol [1-3]. When a commercially feasible method of obtaining eugenol from lignin is developed, the price of eugenol will decrease significantly.

Chapter 3 presents a novel biocomposite from tall oil-based polyamide and lignin-cellulose fiber. The thermal, rheological, and mechanical properties of this biocomposites system were investigated. It was found that LCF can decrease the cost and reinforce the polyamide matrix.

4.2 Recommendation for future works

Many future researches can be performed by extending the results presented in Chapter 2. First of all, the objective of the work presented in Chapter 2 is to develop vegetable oil-based thermoset for pultrusion process. Glass fibers reinforced composites should be produced in the future using the AESO/ME copolymer as the matrix material. Trials on a pultrusion machine should also be performed. In addition, silane coupling agents are effective in increase the adhesion between the glass fiber and matrix, thus leading to composites with higher mechanical properties [4, 5]. The effectiveness of silane coupling agents on the AESO/ME resin system can be investigated in the future. In addition, various fibers can be incorporated into this resin, including carbon fibers, boron fibers, and Kevlar fibers. Natural fibers such as jute, flax, kenaf, and bamboo fibers can also be used.

A systematic curing kinetics study can also be performed on this resin system so that an ideal curing profile can be developed. Even though a long curing schedule is presented in Chapter 2, the purpose of this long curing profile is to make sure the samples are fully cured. Knowledge of curing kinetics will be essential for large-scale manufacturing. The samples prepared in this study were cured in the oven with an open silicon mold; however, it is commonly known that free radical initiators can be inhibited by oxygen and moisture. Unfortunately, curing at an environment free of oxygen and moisture is not achievable with the equipments in my lab. A material with higher mechanical properties can be produced if it is cured in an inert atmosphere. On the other hand, the benzoyl peroxide free radical initiator used in this study is a solid form at room temperature. Since it is a solid, it takes a significant amount of time to dissolve it in the reaction mixture. The effectiveness of various liquid-form free radical initiators in this resin system should also be investigated in the future.

The ASEO/ME polymers are stiff and rigid, but it is relatively brittle. Methods to increase the ductility of this resin system without sacrificing strength and modulus should be developed. To further increase the stiffness and strength of the vegetable oil/ME system, linseed oil and tung oil can be used instead of soybean oil. Linseed oil and tung oil contain more carbon-carbon bond more their fatty acid chains compared to soybean oil. If acrylated epoxidized linseed oil and acrylated epoxidized tung oil can be produced and copolymerized with ME, the stiffness and strength of the composites will increase significantly. Moreover, the AESO and be further modified to increase the stiffness. Anhydride such as maleic anhydride, methacrylic anhydride [6], and have been used to increase the unsaturation sites on AESO. In addition, nanoclay, carbon nanotube,

graphene, boron nitride and other fillers can be added to this resin to produce composites with special properties.

The current procedure of synthesizing ME requires extensive washing. After Methacrylic anhydride reacts with eugenol, methacrylated eugenol and methacrylic acid are produced. Depending on the amount of methacrylic anhydride added, residual unreacted methacrylic anhydride can also be found. The washing technique presented in Chapter 2 was set up to remove the methacrylic acid and the residual methacrylic anhydride. In fact, methacrylic acid also contains carbon-carbon double bonds, and it can act as a copolymer in free radical polymerization. The residual methacrylic anhydride can also be treated as a copolymer. The other way to utilize the methacrylic acid and the residual methacrylic anhydride is to use them to react with epoxidized soybean oil (ESO) or other epoxidized vegetable oils. Methacrylated epoxidized vegetable oils can be formed in this way. In addition, methacrylic anhydride can also react with epoxy rings on the epoxidized vegetable oils and the hydroxyl groups on the ring-opened methacrylated epoxidized vegetable oils. On the other hand, instead of using methacrylic anhydride to modify eugenol, other cheaper anhydride such as maleic anhydride and phthalate anhydride can also be used.

For the PA/LCF biocomposites presented in Chapter 3, modification on the LCF fibers can be performed so that the interfacial adhesion between the polyamide matrix and the LCF fibers can be increased. Other bio-based fillers can also be used to reinforce polyamide.

4.3 References

[1] Telysheva G, Dobele G, Meier D, Dizhbite T, Rossinska G, Jurkjane V. Characterization of the transformations of lignocellulosic structures upon degradation in planted soil. J Anal Appl Pyrol. 2007;79(1-2):52-60.

[2] Kuroda KI, Inoue Y, Sakai K. Analysis of Lignin by Pyrolysis-Gas Chromatography .1. Effect of Inorganic Substances on Guaiacol-Derivative Yield from Softwoods and Their Lignins. J Anal Appl Pyrol. 1990;18(1):59-69.

[3] Varanasi P, Singh P, Auer M, Adams PD, Simmons BA, Singh S. Survey of renewable chemicals produced from lignocellulosic biomass during ionic liquid pretreatment. Biotechnol Biofuels. 2013;6.

[4] Cui HY, Kessler MR. Pultruded glass fiber/bio-based polymer: Interface tailoring with silane coupling agent. Compos Part a-Appl S. 2014;65:83-90.

[5] Cui HY, Kessler MR. Glass fiber reinforced ROMP-based bio-renewable polymers: Enhancement of the interface with silane coupling agents. Compos Sci Technol. 2012;72(11):1264-72.

[6] Adekunle K, Akesson D, Skrifvars M. Synthesis of Reactive Soybean Oils for Use as a Biobased Thermoset Resins in Structural Natural Fiber Composites. J Appl Polym Sci. 2010;115(6):3137-45.